AD 200210

HEAT TRANSFER TO SKIN THROUGH THERMALLY-IRRADIATED DRY CLOTH

Technical Report No. 6

from

Fuels Research Laboratory
Massachusetts Institute of Technology
Cambridge, Massachusetts

Project DSR 7666

Prepared by: N. Y. Chen
W. P. Jensen

Approved by: G. C. Williams

Contract Nonr-1841 (37)
Project No. NR 051-237
Office of Naval Research
Navy Department

July 8, 1958

CONTENTS

Figures 12 through 18: Temperature History Within an Opaque Semi-Infinite Solid (Skin) Following Thermal Irradiation through an Overlying Cloth Layer (Curve I- All Radiation Absorbed at $X_c^o = 0$)

Figures 19 through 25: Temperature History within an Opaque Semi-Infinite Solid (Skin) Following Thermal Irradiation through an overlying Cloth Layer. (Curve II - All Radiation Absorbed at $X_c^o = 0.75$)

Figure 26: Temperature History within an Opaque Semi-Infinite Solid (Skin) Following Thermal Irradiation through an Overlying Cloth Layer (Curve III - All Radiation Absorbed at Skin Surface)

Figure 27: Comparison of Theoretical and Experimental Temperature Histories Within a Skin Simulant Following Thermal Irradiation through Overlying Diathermanous Cloth.

ACKNOWLEDGMENT

The work reported here was supported by the Office of Naval Research, Department of the Navy, in connection with contracts Nonr-1841(00) and Nonr-1841(37) for the study of the protective effects of cloth against damage to skin by thermal radiation. It was also supported by the Quartermaster Research and Engineering Command, Department of the Army, under Contract No. DA-19-129-QM-454, for studies of the mechanism of heat transfer through textiles.

The authors gratefully acknowledge the guidance of Professors Hoyt C. Hottel and Glenn C. Williams throughout this work.

During the early analytical studies Mr. Yves Kersale made a significant contribution by his careful, accurate desk-calculator work.

The aid of the staff of the M.I.T. Computation Center and in particular that of Miss Katherine Kavanaugh was also very valuable.

Finally, the careful typing of a difficult manuscript by Miss Ruth Roland is much appreciated.

ABSTRACT

An analysis is presented of the problem of heat transmission through dry opaque or diathermanous cloth and an air space into underlying skin, following exposure to thermal radiation. The problem is solved numerically by finite difference approximations, the method being given in detail. It is shown that a technique requiring only the appropriate weighting of temperature-rise data obtained from three curves yields results within 1 to 2% of those obtained by extensive machine calculations in which allowance is made for energy absorption at each of several increments into which the diathermanous cloth is conceptually divided. The analytical work is verified by good agreement with experimental results.

I. INTRODUCTION

An experimental research program carried on in the Fuels Research Laboratory during the past two years has focussed on development of skin simulants and their use to obtain temperature-time-depth data in complex multi-layer systems, such as skin behind various dry or moisture-bearing fabrics. A parallel theoretical program was a study of the unsteady-state heat conduction through such multi-layer systems. The role played by the fabrics in heat and mass transfer when exposed to high intensity thermal radiation is probably very complex due both to the inherent heterogeneity of the structure of all fabrics and to the interaction of energy and mass transfer due to moisture in the cloth. However, it is quite possible that, based on the experimental temperature-time-depth data obtained from skin simulant studies, a set of simplifying assumptions might be made to describe adequately the complex model, so that a mathematical analysis can be carried out. This report is concerned only with the problem of heat transfer through dry cloth to skin. The additional complexity due to moisture in the cloth is presently under active study.

A previous attempt at this type of mathematical analysis was made by Ho and Williams (1) in connection with study of an air-spaced cloth-polyethylene system. They tried to correlate experimentally-determined temperatures of the top cloth surface, the bottom cloth surface, and the polyethylene surface with the respective calculated temperatures. Unfortunately, due to slight errors in their theoretical equations, use of erroneous values of cloth conductivity and effects of uncontrolled moisture and chemical reaction in the experiments, their results were far from expectation, and for a time discouraged further attempts at analysis. Their mathematical analysis was based on the assumption that the cloth layer could be treated as a homogeneous solid, which might be a fair approximation for the underlying polyethylene or other skin simulant, but not for the

cloth layer itself. Therefore the analysis could hardly be expected to predict temperature profiles in the cloth layer. Furthermore, the complexity of the cloth structure makes it impossible to identify accurately the cloth "surface", and consequently the significance of experimentally measured temperatures was ambiguous at best.

Since the main interest is to obtain temperature-time patterns at various depths of skin, and since now it is possible to obtain these data experimentally by the use of skin simulants with depth magnification,[2] it seems logical that the theoretical analysis should be directed toward calculating temperature-time data within the simulated skin rather than in the overlying cloth layer. With this purpose in mind, the present work was initiated. The study consists of the correction and modification of Ho and Williams' work, the extension of the analysis to cover both opaque and diathermanous cloths, a proposed modification of the Schmidt technique for calculating unsteady-state heat conduction through heterogeneous systems, the use of a "three-curve" method in solving diathermanous cloth problems, and the use of an IBM-704 computer in calculating the numerical data over the range of interest.

II ANALYSIS OF HEAT TRANSFER IN CLOTH-AIR-SKIN SYSTEMS

A. General Assumptions.

The system under consideration is sketched below.

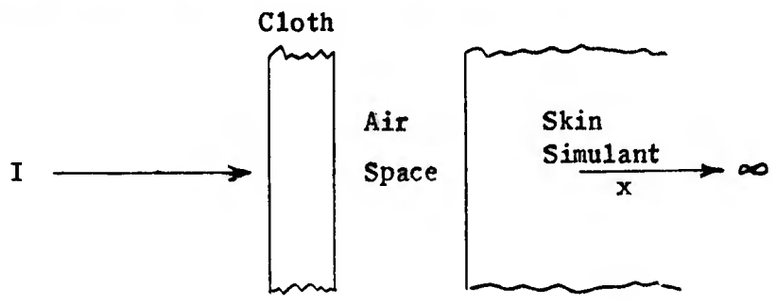

Figure 1.

The following assumptions are made in the analysis:

1. Heat flow is uni-dimensional, occurring in the x-direction, from the cloth through the air space into the skin simulant. The surface of the cloth is irradiated by square wave radiation of uniform intensity.

2. The cloth layer, of thickness L_c is considered to be a homogeneous opaque solid for cloth for which no measurable transmittance has been reported, and for cloth of finite transmittance the radiant energy is assumed to penetrate into the interior of the cloth layer in accordance with the Beer-Lambert Law:

$$I_x = I_o e^{-\gamma x_c} \tag{1}$$

where I_x = intensity of radiation at a plane distant x_c cm. from the irradiated surface,

I_o = intensity of radiation entering the cloth layer, cal/cm^2 sec.,

γ = extinction coefficient, cm^{-1}, a characteristic constant of the cloth for the particular source of radiation in question.

This assumption is made with reference to the particular series of cloths under study in the experimental program at this laboratory. These cloths, ranging in shade from white to deep black, are made from the same white 9-ounce cotton sateen stock, and have measured transmittance values ranging from 0 to 14.1%. Since it is unlikely that a simple dyeing process would change the geometry of the fibers, it is reasonable to assume that the cloth construction provides complete geometrical blockage of incident light and that the transmittance depends on the degree of opacity of the individual cloth fibers. These transmittance values are therefore regarded not as direct transmittance but as diathermancy, as stated in the assumption.

In section V of this report a general method for solving problems of heat transmission through cloth, an air space, and underlying skin is proposed; it

can be applied to either diathermanous cloth samples or to those which allow direct transmission of radiant energy.

3. The physical properties of the cloth layer remain constant throughout the exposure.

4. Any effects due to moisture and/or chemical reaction are negligible.

5. Heat losses from the front surface of the cloth layer, by convection and re-radiation, are characterized by a single overall heat transfer coefficient U_o.

6. Heat transfer from the cloth layer through the air gap to the simulant is similarly characterized by an overall heat transfer coefficient U_i.

7. The skin simulant is considered to be a homogeneous opaque solid, of infinite extent in its x-direction.

B. Derivation of Equations for an Opaque-Cloth, Air, Skin-Simulant System.

Consider the element dx_c in the cloth layer.

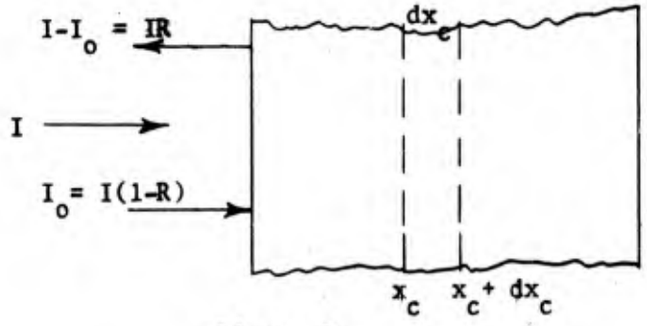

Figure 2.

Per unit area, the rate of heat input at x_c is

$$-k_c \frac{\partial T}{\partial x_c} \tag{2}$$

the rate of heat output at $x_c + dx_c$ is:

$$-k_c \frac{\partial T}{\partial x_c} + \frac{\partial}{\partial x_c}\left(-k_c \frac{\partial T}{\partial x_c}\right) dx_c \tag{3}$$

The heat accumulation in dx_c is:

$$(c\rho)_c \, dx_c \, \frac{\partial T}{\partial \theta_c} \tag{4}$$

Since input minus output equals accumulation, we have:

$$k_c \frac{\partial^2 T}{\partial x_c^2} = (c\rho)_c \frac{\partial T}{\partial \theta_c} \tag{5}$$

Similarly, for the skin simulant, which is an opaque solid, the heat accumulation is:

$$k_s \frac{\partial^2 T}{\partial x_s^2} = (c\rho)_s \frac{\partial T}{\partial \theta_s} \tag{6}$$

The boundary conditions are:

1. At the front surface of the cloth,

$$I_o - U_o \left(T_{x_c = o} - T_{surr.}\right) = -k_c \frac{\partial T}{\partial x_c}\Bigg]_{x_c = 0} \tag{7}$$

2. In the air gap between the cloth and the skin simulant, neglecting the heat capacity of the air,

$$-k_c \frac{\partial T}{\partial x_c}\Bigg]_{x_c = L_c} = U_i\left(T_{x_c = L_c} - T_{x_s = 0}\right) = -k_s \frac{\partial T}{\partial x_s}\Bigg]_{x_s = 0} \tag{8}$$

These nonlinear boundary conditions make the exact solutions of the partial differential equations (5) and (6) unobtainable. Hence the method of finite difference approximations commonly known as the Schmidt method is used. Some modifications of the original Schmidt technique have been made to give answers closer to the exact solution, as will be explained in the next section.

III. FINITE DIFFERENCE APPROXIMATION METHOD

Expressing the above-mentioned differential equations and boundary equations in finite increment terms, we have:

$$k_c \frac{\Delta_x(\Delta_x T)}{\Delta x_c^2} = (c\rho)_c \frac{\Delta_\theta T}{\Delta \theta_c} \qquad (5)'$$

$$k_s \frac{\Delta_x(\Delta_x T)}{\Delta x_s^2} = (c\rho)_s \frac{\Delta_\theta T}{\Delta \theta_s} \qquad (6)'$$

$$I_o - U_o\left(T_{x_c = 0} - T_{surr.}\right) = -k_c \frac{\Delta_x T}{\Delta x_c}\Bigg]_{x_c = 0} \qquad (7)'$$

$$-k_c \frac{\Delta_x T}{\Delta x_c}\Bigg]_{x_c = L_c} = U_i\left(T_{x_c = L_c} - T_{x_s = 0}\right) = -k_s \frac{\Delta_x T}{\Delta x_s}\Bigg]_{x_s = 0} \qquad (8)'$$

Multiplying equation (5)' by $\frac{1}{I_o L_c} \Big/ \left(\frac{1}{L_c}\right)^2$, we obtain

$$\frac{\Delta_x\left(\frac{\Delta_x T k_c}{I_o L_c}\right)}{\Delta\left(\frac{x_c}{L_c}\right)^2} = \frac{\frac{k_c \Delta_\theta T}{I_o L_c}}{\left(\frac{k}{c\rho}\right)_c \left(\frac{1}{L_c}\right)^2 \Delta\theta_c} \qquad (9)$$

A. General equations in dimensionless forms.

To make the solution applicable to problems involving the same system but having different physical constants, the basic equations derived in Section II are transformed into dimensionless forms.

It is convenient to define the dimensionless groups as follows:

$T^o = \frac{Tkc}{I_o L_c}$, the dimensionless temperature group;

$x_c^o = \frac{x_c}{L_c}$, the dimensionless distance group, measured from the front surface of the cloth; and

$\theta_c^o = \left(\frac{k}{c\rho}\right)_c \frac{\Delta\theta_c}{L_c^2}$, the dimensionless time group

Thus, equation (9) can be rewritten as:

$$\frac{\Delta_x\left(\Delta_x T^o\right)}{\Delta\left(x_c^o\right)^2} = \frac{\Delta_\theta T^o}{\Delta\theta_c^o} \qquad (9)$$

Equation (6)' multiplied by the term $\frac{k_c}{I_o L_c} / \left(\frac{1}{L_c}\right)^2$ yields:

$$\frac{\Delta_x\left(\frac{\Delta_x Tk_c}{I_o L_c}\right)}{\Delta\left(\frac{x_s}{L_c}\right)^2} = \frac{\frac{\Delta_\theta Tk_c}{I_o L_c}}{\left(\frac{k}{c\rho}\right)_s \frac{\Delta\theta_s}{L_c^2}} \qquad (10)$$

The dimensionless skin-depth group is defined as:

$$x_s^o = \frac{x_s}{L_c} \cdot \frac{k_c}{k_s}$$

and consequently, from equation (10)

$$\theta_s^o = \left(\frac{k}{c\rho}\right)_s \cdot \frac{\theta_s}{L_c^2} \cdot \left(\frac{k_c}{k_s}\right)^2$$

is the definition of the dimensionless time group for the skin layer.

When both sides of equation (10) are multiplied by $\frac{1}{(k_c/k_s)^2}$ it can be re-written as $\frac{\Delta_x\left(\Delta_x T^o\right)}{\Delta\left(x_s^o\right)^2} = \frac{\Delta_\theta T}{\Delta\theta_s^o}$ (10)'

Boundary equation (7)' can be rearranged as

$$\left.\frac{\Delta_x T}{\Delta x_c}\right]_{x_c=0} = -\frac{I_o}{k_c} + \frac{U_o}{k_c}\left(T_{x_c=0} - T_{surr.}\right)$$

Multiplying both sides by $\left(\frac{k_c}{I_o L_c}\right) / \left(\frac{1}{L_c}\right)$, we obtain

$$\left.\frac{\frac{\Delta_x T\ k_c}{I_o\ L_c}}{\Delta\left(\frac{x_c}{L_c}\right)}\right]_{x_c=0} = -1 + \frac{U_o\ L_c}{k_c}\left[\frac{k_c\ T_{x_c=0}}{I_o\ L_c} - \frac{k_c\ T_{surr.}}{I_o\ L_c}\right] \qquad (11)$$

If a dimensionless surface-heat-loss group, U_o^o, is defined as $\frac{U_o\ L_c}{k_c}$, equation (11) can be rewritten as:

$$\left.\frac{\Delta T^o}{\Delta X_c^o}\right]_{X_c^o = 0} = -\frac{\frac{1}{U_o^o} - \left(T^o_{X_c^o = 0} - T^o_{surr.}\right)}{\frac{1}{U_o^o}} \qquad (11)$$

Similarly, if the air gap group U_i^o is defined in dimensionless terms as $\frac{U_i\ L_c}{k_c}$ boundary equation (8) can be converted to:

$$-\left.\frac{\Delta T^o}{\Delta X_c^o}\right]_{X_c^o = 1} = \frac{T^o_{X_c^o = 1} - T^o_{X_s^o = 0}}{\frac{1}{U_i^o}} = -\left.\frac{\Delta_x T}{\Delta X_s^o}\right]_{X_s^o = 0} \qquad (12)$$

In summarizing the above general equations, it is found that seven dimensionless groups govern the temperature-time-depth pattern of the system, namely

1. Temperature group, $T^o = \frac{k_c T}{I_o L_c}$

2. Time group for cloth $\theta_c^o = \left(\frac{k}{c\rho}\right)_c \left(\frac{\theta_c}{L_c^2}\right)$

3. Time group for skin $\theta_s^o = \left(\frac{k}{c\rho}\right)_s \frac{\theta_s}{L_c^2}\left(\frac{k_c}{k_s}\right)^2$

4. Depth group for cloth $X_c^o = \frac{x_c}{L_c}$

5. Depth group for skin $X_s^o = \frac{x_s}{L_c}\ \frac{k_c}{k_s}$

6. Surface heat losses group $\quad U_o^o = \dfrac{U_o L_c}{k_c}$

7. Air gap group, $\quad U_i^o = \dfrac{U_i L_c}{k_c}$

A relationship between the thermal properties of the cloth and skin would make it possible to eliminate the time and depth groups for skin. In establishing this relationship, the following rules are observed in order to simplify the mathematical manipulations:

1. The modulus, M, defined as $\dfrac{\Delta(x^o)^2}{\Delta\theta^o}$ is to be the same in both the skin and the cloth, and

2. The actual time θ (in seconds) is to be the same in both the skin and the cloth, i.e., $\theta_c = \theta_s$.

$$\text{Thus} \quad \frac{\Delta(x_c^o)^2}{\Delta\theta_c^o} = \frac{\Delta(x_s^o)^2}{\Delta\theta_s^o} \tag{13}$$

and by substitution

$$\frac{\Delta x_c^o}{\Delta x_s^o} = \frac{\sqrt{\left(\dfrac{k}{c\rho}\right)_c \dfrac{\theta_c}{L_c^2}}}{\sqrt{\left(\dfrac{k}{c\rho}\right)_s \left(\dfrac{k_c}{k_s}\right)^2 \dfrac{\theta_s}{L_c^2}}} = \sqrt{\frac{(kc\rho)_s}{(kc\rho)_c}} \tag{14}$$

From equation (14) it is seen that by using cloth as the reference material, the corresponding size of each increment in the skin simulant is inversely proportional to the square root of the kcρ ratio of skin and cloth.

The reason for defining X_s^o as $x_s k_c / L_c k_s$ instead of simply x_s/L_c can be best explained by making a heat balance at the interface of a composite slab, sketched in Figure 3.

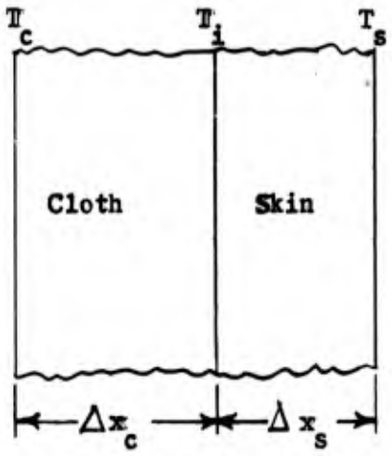

Figure 3.

The boundary condition requires the heat fluxes to be equal at the interface, or:

$$\frac{k_c}{\Delta x_c}(T_c - T_i) = \frac{k_s}{\Delta x_s}(T_i - T_s) \qquad (15)$$

Letting $R = \frac{\Delta x_c}{\Delta x_s} \cdot \frac{k_s}{k_c}$, we have,

$$T_i = \left(\frac{1}{1+R}\right) T_c + \left(\frac{R}{1+R}\right) T_s \qquad (16)$$

If the dimensionless depth groups are defined in such a way that $\Delta X_c^o / \Delta X_s^o = R$, then T_i in equation (16) can be evaluated graphically by drawing a straight line connecting T_c and T_s as shown in Fig. 4. Therefore, when X_c^o is defined as X_c/L_c, it follows that X_s^o should be $\frac{X_s}{L_c} \cdot \frac{k_c}{k_s}$ instead of $\frac{X_s}{L_c}$.

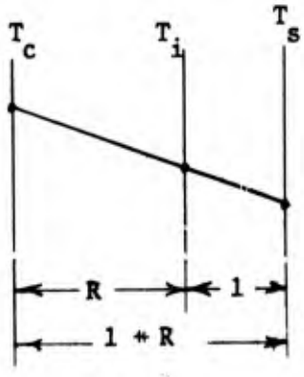

Figure 4.

B. Numerical Solution - Modified Schmidt Technique.

The solution of equations (9)' and (10)' with the boundary conditions set by equations (11)' and (12)' can best be illustrated by working out an actual case.

1. The independent variables U_o^o, U_i^o, and the ratio R (equivalent to $\Delta X_c^o / \Delta X_s^o$ or $\sqrt{\frac{(kc\rho)_s}{(kc\rho)_c}}$ must be assigned for each particular case. For the example, let us say $U_o^o = 0.1$; $U_i^o = 1.0$; $R = 5.0$.

2. With the cloth layer as the reference material, it is convenient to divide the cloth layer into two increments or slices. Each cloth slice, ΔX_c^o, is therefore 0.5 dimensionless units thick and each skin slice, ΔX_s^o, is accordingly 0.1 unit.

In the Schmidt technique reference planes for temperature are located at the center of the slices and also half a slice beyond the surfaces of cloth and skin as shown in Figure 5. This procedure, devised by Schmidt and discussed by McAdams (3) yields an improved approximation of the true solution, over that which would be obtained without the concept of half-slices beyond the surfaces.

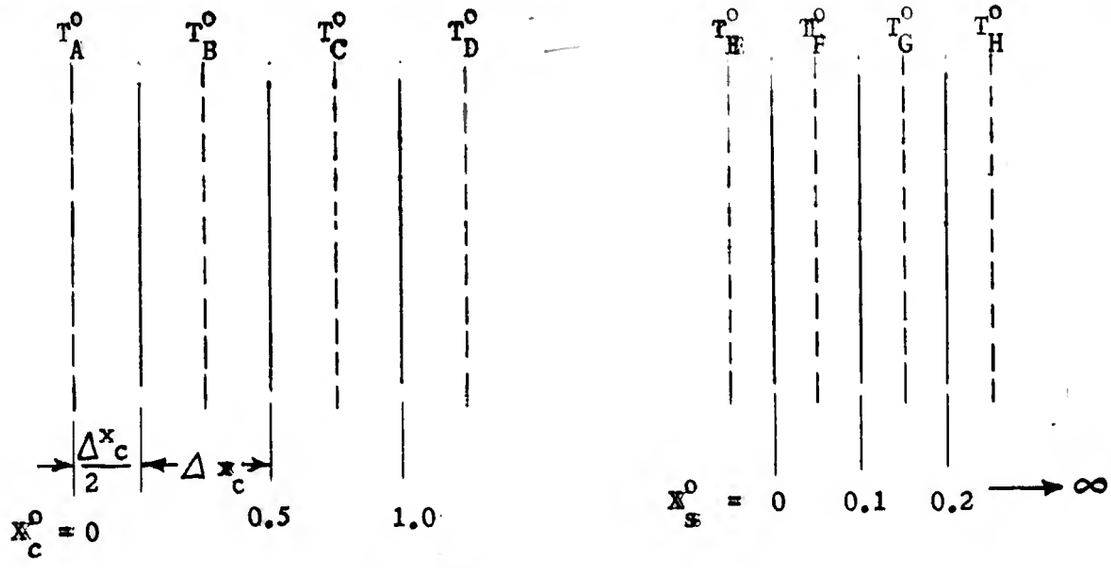

Figure 5.

3. The solution is started by considering boundary equation (11)'

$$\left.\frac{\Delta T^o}{\Delta X_c^o}\right]_{X_c^o = 0} = - \frac{\frac{1}{U_o^o} - \left(T^o_{X_c^o = 0} - T^o_{surr.}\right)}{\frac{1}{U_o^o}} \qquad (11)'$$

Referring to Figure 5,

$$\text{Let } \frac{T_A^o + T_B^o}{2} = T^o_{X_c^o = 0}; \; T_{surr.} = 0; \text{ and } - \frac{(T_A^o - T_B^o)}{\Delta X_c^o} = \left.\frac{\Delta_x T^o}{\Delta X_c^o}\right]_{X_c^o = 0}$$

Equation (11)' can be re-written as:

$$\frac{T_A^o - T_B^o}{\Delta X_c^o} = \frac{2/U_o^o - T_A^o - T_B^o}{2/U_o^o} \tag{17}$$

Rearranging equation (17), we obtain

$$T_A^o = \frac{\Delta X_c^o \left(\frac{1}{U_o^o} - T_B^o\right) + \frac{\Delta X_c^o}{2} T_B^o + \frac{1}{U_o^o} T_B^o}{\frac{1}{U_o^o} + \frac{\Delta X_c^o}{2}} \tag{18}$$

$$= \frac{\Delta X_c^o \left(\frac{1}{U_o^o} - T_B^o\right)}{\frac{1}{U_o^o} + \frac{\Delta X_c^o}{2}} + T_B^o \tag{18}'$$

or in another form,

$$\frac{T_A^o - T_B^o}{\Delta X_c^o} = \frac{\frac{1}{U_o^o} - T_B^o}{\frac{1}{U_o^o} + \frac{\Delta X_c^o}{2}}$$

Equation (18)' is shown graphically in Fig. 6 by connecting the point O of the cloth surface with plane B at the point where $T_B^o = 0$. This line crosses plane A and establishes the starting T_A^o at $\theta_c^o = 0$.

After $T_{A,O}^o$ (the first subscript denotes the temperature plane, and the second a dimensionless time unit) is obtained, the temperature distribution pattern inside the cloth layer is calculated by the use of equation (9)',

$$\frac{\Delta_x \left(\Delta_x T^o\right)}{\Delta \left(X_c^o\right)^2} = \frac{\Delta_\theta T^\phi}{\Delta \theta_c^o} \tag{9}'$$

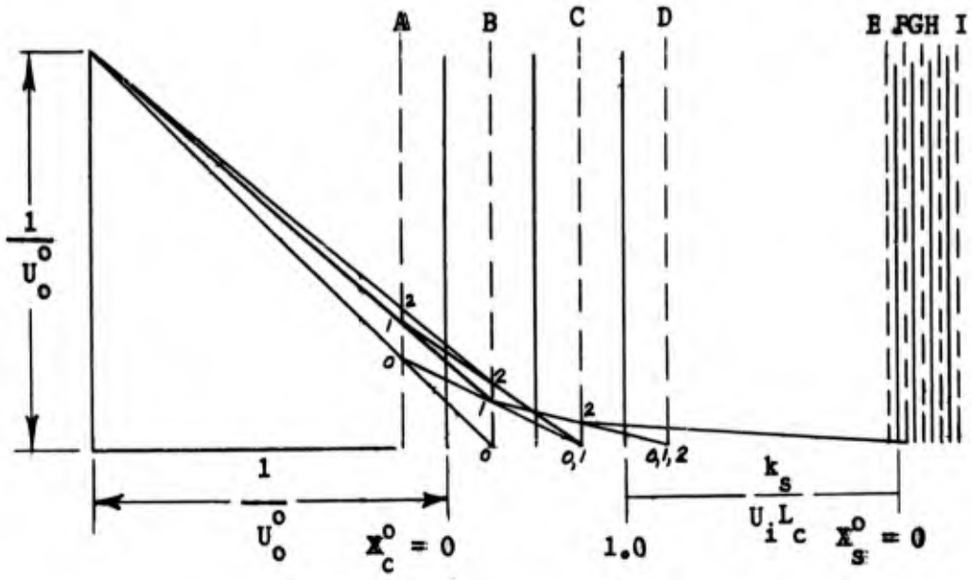

Figure 6.

For plane B, at time unit 1, equation (8)' can be written as

$$(T^o_{C,0} - T^o_{B,0}) - (T^o_{B,0} - T^o_{A,0}) = \frac{\Delta\left(X^o_c\right)^2}{\Delta\theta^o_c}\left(T^o_{B,1} - T^o_{B,0}\right) \qquad (19)$$

Both the dimensionless depth group and the dimensionless time group are independent variables, the choice of their values being entirely arbitrary. But considerable simplification in the arithmetic manipulation is possible if $\Delta\left(X^o_c\right)^2/\Delta\theta^o_c$ is chosen to be 2 as recommended by Schmidt because this causes $T^o_{B,0}$ terms to be cancelled in equation (18), leaving:

$$T^o_{B,1} = \frac{T^o_{A,0} + T^o_{C,0}}{2} \qquad (20)$$

Equation (20) is represented on Figure 6 as a straight line drawn from $T^o_{A,0}$ on plane A to the datum point on plane C; the line crosses plane B, and establishes $T^o_{B,1}$.

Equation (20) can be written in the general form:

$$T^o_{n,m+1} = \frac{T^o_{n-1,m} + T^o_{n+1,m}}{2} \qquad (21)$$

This equation can be used alone until heat reaches the back surface of the cloth, i.e., when in this example T^o_C becomes finite. Then the heat transfer

through the air gap would begin and boundary equation (12)' must be considered. Summarizing, the equations used in the calculation of this example can be expressed by the following algebraic forms, from equations (18)' and (21):

$$T^{o}_{A,m} = 0.04878\ (10 - T^{o}_{B,m}) + T^{o}_{B,m} \quad \text{and}$$

$$T^{o}_{n,m+1} = 0.5\ (T^{o}_{n-1,m} + T^{o}_{n+1,m})$$

It is to be noted here that the foregoing starting technique is different from that suggested by Schmidt. The main difference between the methods lies in the way of fulfilling boundary equation (11)':

$$\left.\frac{\Delta_x T^{o}}{\Delta X^{o}_{c}}\right]_{X^{o}_{c}=0} = -\frac{\frac{1}{U^{o}_{o}} - \left(T^{o}_{X^{o}_{c}=0} - T^{o}_{surr.}\right)}{1/U^{o}_{o}} \qquad (11)'$$

Schmidt pointed out that at time 0, $T^{o}_{X^{o}_{c}=0} = T^{o}_{surr.}$, so that

$$\left.\frac{\Delta_x T^{o}}{\Delta X^{o}_{c}}\right]_{X^{o}_{c}=0} = -\frac{1/U^{o}_{o}}{1/U^{o}_{o}} = -1 \qquad (22)$$

This is represented graphically in Figure 7 by the line which connects the starting point with the point where $X^{o}_{c} = 0$ and $T^{o} = T^{o}_{o}$. This line establishes T^{o}_{A} for the starting time $\theta^{o} = 0$ at the point where it crosses plane A. Schmidt's procedure for continuation to determine T^{o}_{B}, etc., has been used in the present work. Comparing the starting procedures shown in Figures 6 and 7, however, it is clear that our method gives a higher value than Schmidt's for $T^{o}_{A,0}$. It is also somewhat closer to the true solution, due to a partial balance of compensating errors. In our approximation of the surface boundary condition, equation (11)', the heat capacity of the half slice of cloth from plane B to the surface

is neglected, which is the same as assuming for the moment that it equals that of air. The error is partially compensated in the next step, determination of $T^o_{B,1}$, in which the air between plane A and the surface is in effect assigned a heat capacity equal to that of cloth. In the Schmidt starting procedure there is no error in the first step but in the second step all the space between planes A and B is implicitly assumed to have the heat capacity of cloth, an error for which no compensation is made.

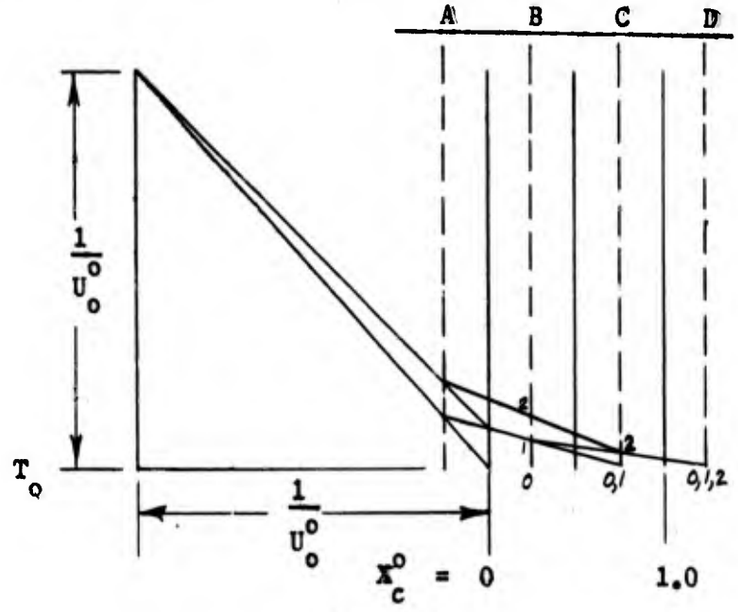

Figure 7.

4. Temperature Rise in Air Gap and Skin Simulant.

From boundary equation (12)' and Figure 5,

$$-\left.\frac{\Delta T^o}{\Delta X^o_c}\right]_{X^o_c = 1} = U^o_i \left(T^o_{X^o_c = 1} - T^o_{X^o_s = 0}\right) = -\left.\frac{\Delta T}{\Delta X^o_s}\right]_{X^o_s = 0} \qquad (12)'$$

Letting $\dfrac{T^o_C - T^o_D}{\Delta X^o_c} = -\left.\dfrac{\Delta T^o}{\Delta X^o_c}\right]_{X^o_c = 1}$ and $\dfrac{T^o_E - T^o_F}{\Delta X^o_s} = -\left.\dfrac{\Delta T^o}{\Delta X^o_s}\right]_{X^o_s = 0}$

it follows that

$$\frac{T_C^o - T_D^o}{\Delta X_c^o} = U_i^o \left(\frac{T_C^o + T_D^o}{2} - \frac{T_E^o + T_F^o}{2} \right) = \frac{T_E^o - T_F^o}{\Delta X_s^o} \tag{23}$$

From equation (23),

$$T_E^o = \Delta X_s^o \left(\frac{T_C^o - T_D^o}{\Delta X_c^o} + \frac{T_F^o}{\Delta X_s^o} \right) \tag{24}$$

and $$\frac{T_E^o + T_F^o}{2} = \frac{\Delta X_s^o}{2} \left(\frac{T_C^o - T_D^o}{\Delta X_c^o} + \frac{2\, T_F^o}{\Delta X_s^o} \right) \tag{25}$$

Substituting equation (25) back to equation (23) and eliminating T_E^o, we obtain

$$\frac{T_C^o - T_D^o}{\Delta X_c^o} = U_i^o \left[\frac{T_C^o + T_D^o}{2} - \left(\frac{T_C^o - T_D^o}{\Delta X_c^o} + \frac{2\, T_F^o}{\Delta X_s^o} \right) \frac{\Delta X_s^o}{2} \right] \tag{26}$$

By rearranging (26), $$T_D^o = \frac{(T_C^o - T_F^o) \left[\frac{1}{U_i^o} + \frac{\Delta X_s^o - \Delta X_c^o}{2} \right]}{\frac{1}{U_i^o} + \left(\frac{\Delta X_s^o + \Delta X_c^o}{2} \right)} + T_F^o \tag{27}$$

or $$\frac{T_D^o - T_F^o}{\frac{1}{U_i^o} + \frac{\Delta X_s^o}{2} - \frac{\Delta X_c^o}{2}} = \frac{T_C^o - T_F^o}{\frac{1}{U_i^o} + \frac{\Delta X_c^o}{2} + \frac{\Delta X_s^o}{2}} \tag{28}$$

The last equation can also be obtained graphically by proportioning two similar triangles, as shown in Fig. 8. Similarly, T_E^o can be calculated by

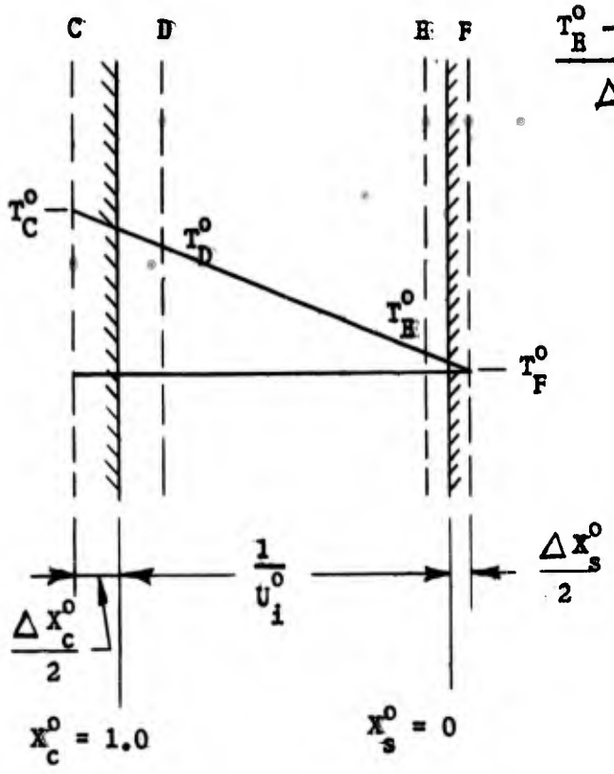

$$\frac{T_E^o - T_F^o}{\Delta X_s^o} = \frac{T_C^o - T_F^o}{\frac{1}{U_i^o} + \frac{\Delta X_c^o}{2} + \frac{\Delta X_s^o}{2}} \qquad (29)$$

Figure 8.

$$\text{or} \quad T_E^o = \frac{(T_C^o - T_F^o)\,\Delta X_s^o}{\frac{1}{U_i^o} + \frac{\Delta X_c^o}{2} + \frac{\Delta X_s^o}{2}} + T_F^o \qquad (30)$$

The advantage of the definition for ΔX_s^o is revealed in the simplicity of the calculation of heat transfer through the air gap. The calculation can also be made graphically, for as can be seen in Figure 8, if the planes $X_c^o = 1$ and $X_s^o = 0$ are separated by a distance corresponding to $\frac{1}{U_i^o}$, equation (12) can be satisfied by a straight line joining plane C and plane F making the heat fluxes at $X_c^o = 1$, $X_s^o = 0$ and $U_i^o \left(T^o_{X_c^o = 1} - T^o_{X_s^o = 0} \right)$ equal to each other. The straight line crosses planes D and E and establishes T_D^o and T_E^o respectively.

Summarizing, the general equations for the two temperature planes inside

the air gap at any time are:

$$\frac{T^o_{D,m} - T^o_{F,m}}{T^o_{C,m} - T^o_{F,m}} = \frac{\frac{1}{U^o_i} + \frac{\Delta X^o_s - \Delta X^o_c}{2}}{\frac{1}{U^o_i} + \frac{\Delta X^o_s + \Delta X^o_c}{2}}$$

$$\text{or } T^o_{D,m} = \frac{\left(T^o_{C,m} - T^o_{F,m}\right)\left[\frac{1}{U^o_i} + \frac{\Delta X^o_s - \Delta X^o_c}{2}\right]}{\frac{1}{U^o_i} + \frac{\Delta X^o_s + \Delta X^o_c}{2}} + T^o_{F,m}; \qquad (31)$$

similarly

$$\frac{T^o_{E,m} - T^o_{F,m}}{T^o_{C,m} - T^o_{F,m}} = \frac{\Delta X^o_s}{\frac{1}{U^o_i} + \frac{\Delta X^o_s + \Delta X^o_c}{2}}$$

$$\text{or } T^o_{E,m} = \frac{\left(T^o_{C,m} - T^o_{F,m}\right)\left(\Delta X^o_s\right)}{\frac{1}{U^o_i} + \frac{\Delta X^o_s + \Delta X^o_c}{2}} + T^o_{F,m}, \qquad (32)$$

In the example,

$$T^o_{D,m} = .6154\ (T^o_{C,m} - T^o_{F,m}) + T^o_{F,m}$$

$$T^o_{E,m} = .07692\ (T^o_{C,m} - T^o_{F,m}) + T^o_{F,m}$$

The final step is conduction of the heat into the interior of the skin simulant. Using equation (10)' and setting $\Delta(X^o_s)^2 / \Delta\theta^o_s = 2$ as in the case of conduction through the cloth layer, the same equation is of course found,

$$T^o_{n,m+1} = \frac{T^o_{n-1,m} + T^o_{n+1,m}}{2} \qquad (21)$$

It is plain that equation (21) can be used throughout the skin simulant, which is treated as a semi-infinite solid.

Accuracy of Solution

It has been well established for this particular type of problem that the solution will converge as long as the modulus $M = \Delta\left(X_c^o\right)^2 / \Delta\theta_c^o$ is equal to 2 or more, and the only question remaining is the accuracy of the solution. It is generally true that an increase in either the modulus or the fineness of the increment would increase the accuracy of the solution. However, any modulus other than 2 would complicate the arithmetic of the problem; therefore varying the number of slices into which the cloth is conceptually divided is a better way to check on the accuracy of the solution.

It is also obvious that the more slices into which the cloth layer is divided, the closer will be the solution to the true solution. However, the number of dimensionless time increments required to arrive at a given corresponding time in seconds is proportional to the square of the number of slices into which the cloth is divided. There is therefore an optimum point in the division of the cloth into small increments, beyond which the precision gained will be small in comparison with the amount of effort required. Experience in performing the calculations with a desk calculator shows that the work becomes extremely long and tedious if one tries to divide the cloth into more than two slices. Thus, it is important to find out how good a two-slice cloth model is as compared with models using more than 2 slices.

With the aid of the IBM-704 digital computer at the MIT Computation Center, it has been possible to check a two-slice solution with a six-slice solution. The results are shown in Tables I and II. From this it is seen that at $\theta_c^o = 2.50$, the difference between the two solutions is less than 1%, while at shorter times, such as $\theta_c^o = 0.5$, the error is over 10%. Using a method commonly given

for estimating the true solution from approximate solutions, and specifically determining T^o_∞ from the 2-slice solution, T^o_2, and the six-slice solution, T^o_6:

$$\frac{T^o_\infty - T^o_2}{T^o_\infty - T^o_6} = \left(\frac{6}{2}\right)^2 ; \qquad (33)$$

when T^o_2 is 10% higher than T^o_6, then

$T_\infty = \frac{9.(1.0) - 1.1}{8} = .9875$, so that the improvement to be expected from an infinite-slice model is less than 1.3%; in other words, very little improvement can be expected if one chooses to use a model having more than 6 cloth increments.

Since $\theta^o_c = 0.5$ corresponds to a little over one second for the 9-ounce cotton sateen being studied in the experimental program here, use of a two-slice model would introduce a serious uncertainty in the short-time region. A compromise solution which can achieve the accuracy of a 6-slice model while requiring only approximately a quarter of the computation time is a combination of the six-slice and the two-slice models., i.e., the computation is started with a 6-slice model and continued until a relatively stable temperature profile prevails inside the skin layer, followed by a shift to a two-slice model using this pre-established temperature profile as the starting condition.

The data in Table I and Table II are also plotted in Fig. 9, and the estimated true solution (Eq. 33) is shown as a dotted line. It is to be noted that the true solution lies above the approximation at shorter times and below the approximation at longer times.

Finally, to test our modification of the Schmidt technique, mentioned in Section III, a calculation was made in which the cloth layer was assumed to be a semi-infinite solid (this would be valid for a short time after the irradiation is started, i.e., before appreciable heat reaches the back side of the

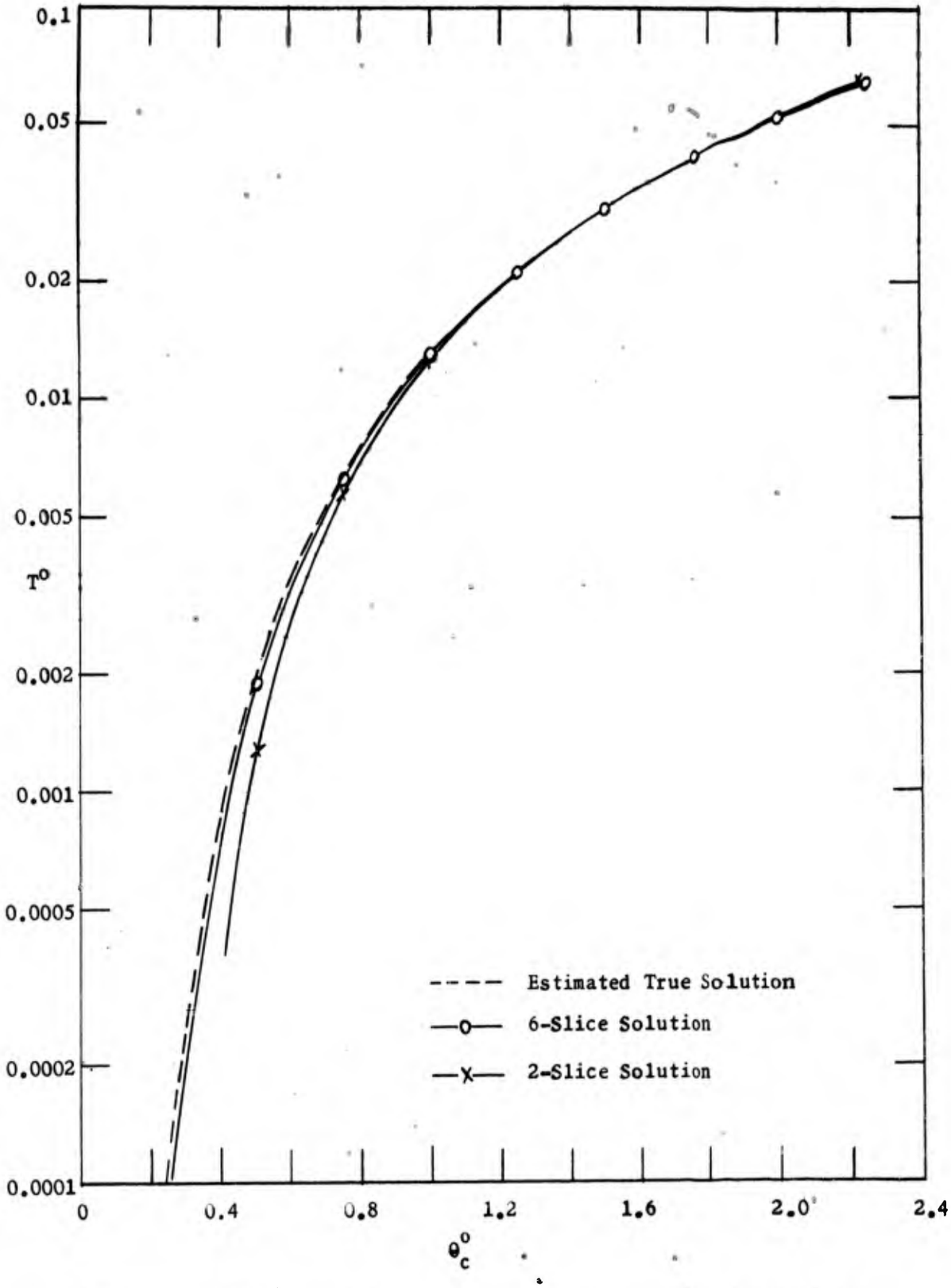

Figure 9. Comparison of Solutions of 2-Slice and 6-Slice Models with Estimated True Solution.

$X_s^o = 0.15$ $\quad U_o^o = 0.04$

$R = 5.0$ $\quad U_i^o = 0.5$

cloth.) From the analytical solution given by Gardon (4) for such a case, the temperature at the time-position values corresponding to the data points of the finite-difference approximation were determined. These data are compared in Table III with the results obtained from the new starting technique and the original Schmidt technique. It is clearly evident the new starting technique is a better approximation of the true solution.

IV. APPLICATION TO DIATHERMANOUS-CLOTH-AIR-SKIN SYSTEMS.

As stated in the general assumptions (Section II, A.), the radiant energy received by a diathermanous cloth layer is assumed to penetrate into the interior of the cloth according to the Beer-Lambert Law. Strictly speaking, this law is applicable to monochromatic radiation only and for most materials, the extinction coefficient, γ, varies with the wave length of the incident radiation. Hence the use of a single extinction coefficient in the present study is merely a first approximation. It is of interest, however, to see how this approximation compares with the experimental results.

With radiation absorbed inside the cloth layer, the differential equation (5) for heat accumulation in the cloth now becomes:

$$-\frac{\partial}{\partial x_c}\left[-k_c\frac{\partial T}{\partial x_c}\right]dx_c - \frac{\partial}{\partial x_c}\left[I_o e^{-\gamma x_c}\right]dx_c = (c\rho)_c\, dx_c \frac{\partial T}{\partial \theta} \qquad (5)''$$

and the boundary condition at the front surface of the cloth becomes

$$-U_o\left(T_{x_c=0} - T_{surr.}\right) = -k_c\frac{\partial T}{\partial x_c}\Big]_{x_c=0} \qquad (7)''$$

Due to the absorption of part of the incident radiation at the surface of the skin simulant, equations for the boundary conditions in the air gap between the cloth and skin simulant have to be rewritten as follows:

(a) Between the back surface of the cloth and the air gap:

$$-k_c \left.\frac{\partial T}{\partial x_c}\right]_{x_c = L_c} = U_i \left(T_{x_c = L_c} - T_{x_s = 0} \right) \qquad (8)$$

(b) Between the air gap and the surface of the skin simulant:

$$I_o e^{-\gamma L_c} - U_i \left(T_{x_s = 0} - T_{x_c = L_c} \right) = -k_c \left.\frac{\partial T}{\partial x_s}\right]_{x_s = 0} \qquad (8)''$$

Before proceeding to solve the above system, it is useful to examine the Beer-Lambert Law graphically:

From eq. (1) $I_x = I_o e^{-\gamma x_c}$ and

$$\ln \frac{I_x}{I_o} = -\gamma L_c \cdot \frac{x_c}{L_c}$$

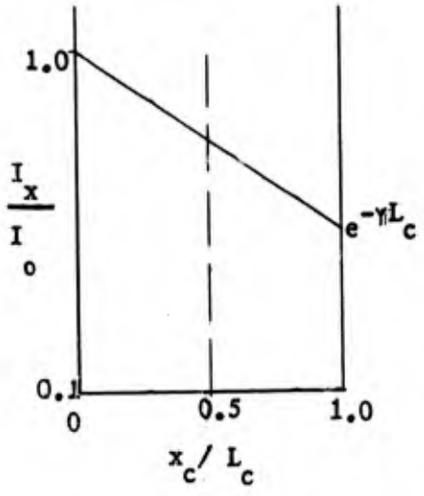

Figure 10.

Therefore, when $\ln I_x/I_o$ is plotted on semi-log paper against x_c/L_c, a straight line should result, with $I_x/I_o = 1$ at $x_c/L_c = 0$, and $I_x/I_o = e^{-\gamma L_c}$ at $x_c/L_c = 1$, as shown in Fig. 10. It should also be noted that $e^{-\gamma L_c}$ is equal to the fraction of the incident radiation absorbed at the surface of the skin, i.e., the measured "transmittance" value divided by one minus the measured reflectance of the cloth or $e^{-\gamma L} = \tau/(1-R)$.

In using the finite-difference approximation method to solve this problem, it is assumed that the amount of radiation absorbed in the center of each finite increment or slice of cloth is distributed according to the above law. For cloth of high diathermancy, the incident radiation intensity as it travels through the cloth decreases nearly linearly with distance and thus justifies

this assumption; but for cloth of low diathermancy, the intensity of radiation drops sharply to a low value at the front part of the cloth. For the latter, it would be a better approximation to assume that the fraction of incident radiation that is absorbed in the first increment of the cloth layer is absorbed at the surface of the cloth (as in the case of an opaque cloth) rather than at the center of that increment.

With the above understanding, Equations (5)', (7)", (8) and (8)" can be re-written in dimensionless finite-increment terms, using the procedures outlined in Section III, to yield the following equations:

1. For the cloth layer:

$$\frac{\Delta_x(\Delta_x T^o)}{\Delta(X_c^o)^2} - \frac{\Delta_x e^{-\gamma L_c X_c^o}}{\Delta X_c^o} = \frac{\Delta_\theta T^o}{\Delta \theta_c^o} \tag{34}$$

2. For the skin simulant:

$$\frac{\Delta_x(\Delta_x T^o)}{\Delta(X_s^o)^2} = \frac{\Delta_\theta T}{\Delta \theta_s^o} \tag{10}$$

3. For the boundary condition at the front cloth surface:

(a) High diathermancy

$$\left.\frac{\Delta_x T^o}{\Delta X_c^o}\right]_{X_c^o = 0} = U_o^o\left(T^o_{X_c^o = 0} - T^o_{surr.}\right) \tag{35}$$

(b) Low diathermancy

$$\left.\frac{\Delta_x T^o}{\Delta X_c^o}\right]_{X_c^o = 0} = -\frac{\frac{1}{U_o^o}\left(\Delta_x e^{-\gamma L_c X_c^o}\right) - \left(T^o_{X_c^o = 0} - T^o_{surr.}\right)}{\frac{1}{U_o^o}} \tag{36}$$

and consequently, the equation for the first increment differs from equation (35) by the absence of the radiation term, i.e.,

$$\frac{\Delta_x(\Delta_x T^o)}{\Delta(x_c^o)^2} = \frac{\Delta_\theta T^o}{\Delta\,\theta_c^o} \tag{9}'$$

4. Boundary conditions in the air gap:

(a) Between the back surface of the cloth and the air gap.

$$\left.-\frac{\Delta_x T^o}{\Delta x_c^o}\right]_{X_c^o = 1} = U_i^o\left(T_{X_c^o=1}^o - T_{X_s^o=0}^o\right) \tag{12}'$$

(b) Between the air gap and the surface of the skin simulant

$$e^{-\gamma L}\,U_i^o\left(T_{X_s^o=0}^o - T_{X_c^o=1}^o\right) = \left.-\frac{\Delta_x T^o}{\Delta X_s^o}\right]_{X_s^o=0}$$

$$\text{or}\quad \left.\frac{\Delta_x T^o}{\Delta X_s^o}\right]_{X_s^o=0} = -\frac{\frac{1}{U_i^o}\left(e^{-\gamma L}\right) - \left(T_{X_s^o=0}^o - T_{X_c^o=1}^o\right)}{\frac{1}{U_i^o}} \tag{37}$$

The numerical solution for this problem is exactly the same as that of an opaque cloth system, except that in the present case, the independent variable γL_c must also be fixed for each particular case. Using the same example as in Section III B, and assigning a value of 2.82 to γL_c (equivalent to $e^{-\gamma L_c} = .06$, as for 9-ounce Medium Gray Cotton Sateen), the above equations become:

$$T_{A,0}^o = \frac{\Delta X_c^o\left(\frac{1}{U_o^o}\,\Delta_x e^{-\gamma L_c X_c^o} - T_{B,0}^o\right)}{\frac{1}{U_o^o} + \frac{\Delta X_c^o}{2}} + T_{B,0}^o \tag{38}$$

$$T^{o}_{B,1} = \frac{T^{o}_{A,0} + T^{o}_{C,0}}{2} \tag{39}$$

$$T^{o}_{C,1} = \frac{T^{o}_{B,0} + T^{o}_{D,0}}{2} - \frac{\Delta_x e^{-\gamma L_c} X^{o}_{c} \left(\Delta X^{o}_{c}\right)}{2} \tag{40}$$

$$T^{o}_{D,0} = \frac{\left(T^{o}_{F,0} - T^{o}_{C,0}\right) \Delta X^{o}_{c} + \frac{\Delta X^{o}_{s} \Delta X^{o}_{c} \cdot e^{-\gamma L_c}}{2}}{\frac{1}{U^{o}_{i}} + \frac{\Delta X^{o}_{s}}{2} + \frac{\Delta X^{o}_{c}}{2}} + T^{o}_{C,0} \tag{41}$$

$$T^{o}_{E,0} = \frac{\left(T^{o}_{E,0} - T^{o}_{C,0}\right)\left(\frac{1}{U^{o}_{i}} + \frac{\Delta X^{o}_{c}}{2} - \frac{\Delta X^{o}_{s}}{2}\right) + \frac{\Delta X^{o}_{c} \Delta X^{o}_{s} \cdot e^{-\gamma L_c}}{2} + \frac{\Delta X^{o}_{s} \cdot e^{-\gamma L_c}}{U^{o}_{i}}}{} + T^{o}_{C,0} \tag{42}$$

$$T^{o}_{F,1} = \frac{T^{o}_{E,0} + T^{o}_{G,0}}{2}, \text{ etc.}$$

To summarize, the algebraic equations used in numerical examples for both the opaque cloth and diathermanous cloth systems are as follows:

1. Size of cloth increment, $\Delta X^{o}_{c} = 0.5$

2. Size of skin increment, $\Delta X^{o}_{s} = 0.1$

3. $U^{o}_{o} = 0.1$, $U^{o}_{i} = 1.0$,

4. The ratio $\sqrt{\frac{(k\rho)_s}{(k\rho)_c}} = 5.0$

5. $e^{-\gamma L_c} = \infty$ for opaque cloth; $e^{-\gamma L_c} = 0.06$, for diathermanous medium grey cloth.

6. Opaque Cloth System	Diathermanous Cloth System
$T^o_{A,m} = .04878(10-T^o_{B,m}) + T^o_{B,m}$	$T^o_{A,m} = .04878(7.55-T^o_{B,m}) + T^o_{B,m}$
$T^o_{B,m+1} = 0.5(T^o_{A,m} + T^o_{C,m})$	$T^o_{B,m+1} = 0.5\ (T^o_{A,m} + T^o_{C,m})$
$T^o_{C,m+1} = 0.5\ (T^o_{B,m} + T^o_{D,m})$	$T^o_{C,m+1} = 0.5(T^o_{B,m} + T^o_{D,m}) + .04625$
$T^o_{D,m} = .6154\ (T^o_{C,m} - T^o_{F,m}) + T^o_{F,m}$	$T^o_{D,m} = .3846\ (T^o_{F,m} - T^o_{C,m}) + T^o_{C,m} + .001154$
	$= .6154\ (T^o_{C,m} - T^o_{F,m}) + T^o_{F,m} + .001154$
$T^o_{E,m} = .0769\ (T^o_{C,m} - T^o_{F,m}) + T^o_{F,m}$	$T^o_{E,m} = .9231\ (T^o_{F,m} - T^o_{C,m}) + T^o_{C,m} + .005769$
	$= .0769(T^o_{C,m} - T^o_{F,m}) + T_{F,m} + .005769$
$T^o_{F,m+1} = 0.5\ (T^o_{E,m} + T^o_{G,m})$	$T^o_{F,m+1} = 0.5\ (T_{E,m} + T^o_{G,m})$

(43 a, b, c, d, e, f)

V. SIMPLIFIED GENERAL SOLUTION FOR SYSTEMS HAVING DIATHERMANOUS CLOTH

From the foregoing discussion, it is seen that the method just introduced would require a complete set of calculations for each value of γL_c. A closer comparison of the equations for the diathermanous cloth with that for the opaque cloth shows that the differences between these two sets of equations involve only the constant terms. Therefore, a general solution for any diathermanous cloth should be possible, if in each of a number of calculations it is assumed that a unit of incident radiant energy is absorbed in one particular increment of the cloth layer. Thus, if the cloth is divided into two increments, only three sets of calculations, and if the cloth is divided into six increments, a total of seven sets of calculations would be necessary. To

get the solution for a cloth having a particular τL_c value, it is only necessary to sum up with proper weighting the solutions of each set of calculations; the weighting is determined by absorption distribution given by the Beer-Lambert Law.

The proposed "three curve" method is an example of this technique. The method requires three sets of solutions, called curves I, II, and III, which differ only in the assumption regarding the location of radiant-energy absorption. Curve I represents the case of a unit of incident radiant energy absorbed at the cloth surface. This is equivalent to the opaque-cloth solution. Curve II represents the case of incident radiant energy absorbed at $X_c^o = 0.75$. Curve III represents the case of incident radiant energy absorbed at the surface of the skin simulant.

Thus it is seen that together with the solution for the opaque cloth system, only two additional sets of solutions are necessary for the general solution of all diathermanous cloth systems. The last two curves are calculated in exactly the same fashion as the first curve, except that in Curve II, the radiant energy is absorbed in the increment whose mid-plane lies on dimensionless depth $X_c^o = 0.75$.

The basic equations in finite difference form become:

1. For the cloth layer,

(a) Any increment other than the increment associated with $X_c^o = 0.75$,

$$\frac{\Delta_x\left(\Delta_x T^o\right)}{\Delta\left(X_c^o\right)^2} = \frac{\Delta_\theta T^o}{\Delta \theta_c^o} \qquad (9)$$

(b) For the cloth increment whose centerline is at $X_c^o = 0.75$,

$$\frac{\Delta_x(\Delta_x T^o)}{\Delta(X_c^o)^2} + \frac{1}{\Delta X_c^o} = \frac{\Delta_\theta T}{\Delta \theta_c^o} \tag{44}$$

2. For the skin simulant

$$\frac{\Delta_x(\Delta_x T)}{\Delta_x(X_s^o)^2} = \frac{\Delta_\theta T}{\Delta \theta_s^o} \tag{10}'$$

3. Boundary conditions in the air gap,

$$-\left.\frac{\Delta_x T^o}{\Delta X_c^o}\right]_{X_c^o = 1} = U_i^o\left(T_{X_c^o = 1} - T_{X_s^o = o}\right) = -\left.\frac{\Delta_x T^o}{\Delta X_s^o}\right]_{X_s^o = 0} \tag{12}'$$

Similarly in curve III, the radiant energy is absorbed at the surface of the skin simulant, and the basic equations are:

1. For the cloth layer,

$$\frac{\Delta_x(\Delta_x T^o)}{\Delta(X_c^o)^2} = \frac{\Delta_\theta T}{\Delta \theta_c^o} \tag{9}'$$

2. For the skin simulant,

$$\frac{\Delta_x(\Delta_x T^o)}{\Delta(X_s^o)^2} = \frac{\Delta_\theta T^o}{\Delta \theta_s^o} \tag{10}'$$

3. Boundary conditions at the front cloth surface,

$$\left.\frac{\Delta_x T^o}{\Delta X_c^o}\right]_{X_c^o = 0} = U_o^o\left(T_{X_c^o = 0} - T_{surr.}^o\right) \tag{35}$$

4. Boundary conditions in the air gap.

(a) Between the back surface of the cloth and the air gap,

$$-\left.\frac{\Delta_x T^o}{\Delta X_c^o}\right]_{X_c^o = 1} = U_i^o \left(T^o_{X_c^o = 1} - T^o_{X_s^o = 0} \right) \qquad (12)$$

(b) Between the air gap and the surface of the skin simulant

$$1 - U_i^o \left(T^o_{X_s^o = 0} - T^o_{X_c^o = 1} \right) = -\left.\frac{\Delta_x T^o}{\Delta X_s^o}\right]_{X_s^o = 0}$$

or

$$-\left.\frac{\Delta_x T^o}{\Delta X_s^o}\right]_{X_s^o = 0} = \frac{\frac{1}{U_i^o} - \left(T^o_{X_s^o = 0} - T^o_{X_c^o = 1} \right)}{\frac{1}{U_i^o}} \qquad (45)$$

Using the same material as before and comparing with equations (43a) to (43 f) inclusive, the equations for curve II are as follows:

$$T^o_{A,m} = .9512\, T^o_{B,m}$$

$$T^o_{B,m} = 0.5\, (T^o_{A,m,} + T^o_{C,m})$$

$$T^o_{C,m+1} = 0.5\, (T^o_{B,m} + T^o_{D,m}) + .2500 \qquad (46\ a, b, c, d, e, f)$$

$$T^o_{D,m} = .6154\, (T^o_{C,m} - T^o_{F,m}) + T^o_{F,m}$$

$$T^o_{H,m} = .0769\, (T^o_{C,m} - T^o_{F,m}) + T^o_{F,m}$$

$$T^o_{F,m+1} = 0.5\, (T^o_{H,m} + T^o_{G,m})$$

Similarly for curve III, the radiant energy is absorbed at the surface of the skin simulant, and the equations are:

$$T^{o}_{A,m} = .9512\ T^{o}_{A,m}$$

$$T^{o}_{B,m+1} = 0.5\ (T^{o}_{A,m} + T^{o}_{C,m})$$

$$T^{o}_{C,m+1} = 0.5\ (T^{o}_{B,m} + T^{o}_{D,m}) \qquad (47\ a, b, c, d, e, f)$$

$$T^{o}_{D,m} = .6154\ (T^{o}_{C,m} - T^{o}_{F,m}) + T^{o}_{F,m} + .01923$$

$$T^{o}_{E,m} = .0769\ (T^{o}_{C,m} - T^{o}_{F,m}) + .09615 + T^{o}_{F,m}$$

$$T^{o}_{F,m+1} = 0.5\ (T^{o}_{E,m} + T^{o}_{G,m})$$

Finally, the solution for any diathermanous-cloth problem can be obtained by summing up these three curves in their proper proportion. These proportionality constants can be obtained either graphically as shown in Fig. 10, or directly from the Beer-Lambert Law. Using the numerical example in which $e^{-\gamma L} = .06$, we have

$$T^{o}_{0.06} = 0.755\ (T^{o}_{I}) + 0.185\ (T^{o}_{II}) + 0.06\ (T^{o}_{III}) \qquad (48)$$

It can be shown that the solution obtained by this method is exactly the same as that calculated by the method described in Section IV.

For highly diathermanous cloth, as mentioned in Section IV, a better approximation would be based on the assumption that radiation is absorbed in the center of each cloth increment. This would seem to necessitate a new curve which can be called Curve I', in place of curve I, which represents surface absorption. However, a closer examination of the two approximations shows that

Curve I and Curve I' are really interrelated, and can be converted from one to the other. The conversion can be best explained by reviewing the basic equations used, as follows:

Figure 11 shows the three temperature planes being considered at the front part of the cloth:

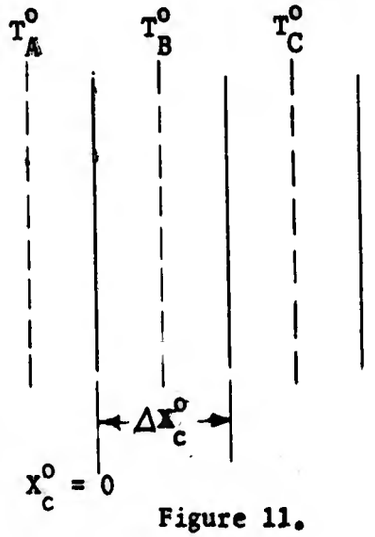

Figure 11.

For curve I, we have:

$$T^o_{A,0} = \frac{\Delta X^o_c \left(\frac{1}{U^o_o} - T^o_{B,0} \right)}{\frac{1}{U^o_o} + \frac{\Delta X^o_c}{2}} + T^o_{B,0}$$

$$= \frac{\frac{\Delta X^o_c}{U^o_o} + \left(\frac{1}{U^o_o} - \frac{\Delta X^o_c}{2} \right) T^o_{B,0}}{\frac{1}{U^o_o} + \frac{\Delta X^o_c}{2}} \qquad (49)$$

$$T^o_{B,1} = \frac{T^o_{A,0} + T^o_{C,0}}{2}$$

Combining these two equations, we obtain:

$$T^o_{B,1} = \frac{\left(\frac{1}{U^o_o} - \frac{\Delta X^o_c}{2} \right) T^o_{B,0}}{2\left(\frac{1}{U^o_o} + \frac{\Delta X^o_c}{2} \right)} + \frac{T^o_{C,0}}{2} + \frac{\Delta X^o_c}{2 + \Delta X^o_c \; U^o_o} \qquad (50)$$

For Curve I', we have,

$$T^o_{A,0} = \frac{\left(\frac{1}{U^o_o} - \frac{\Delta X^o_c}{2} \right) T^o_{B,0}}{\frac{1}{U^o_o} + \frac{\Delta X^o_c}{2}} \qquad (51)$$

$$T^o_{B,1} = \frac{T^o_{A,0} + T^o_{C,0}}{2} + \frac{\Delta X^o_c}{2}$$

Combining these two equations, we obtain,

$$T^o_{B,1} = \frac{\left(\frac{1}{U^o_o} - \frac{\Delta X^o_c}{2}\right) T^o_{B,0}}{2\left(\frac{1}{U^o_o} + \frac{\Delta X^o_c}{2}\right)} + \frac{T^o_{C,0}}{2} + \frac{\Delta X^o_c}{2} \qquad (52)$$

The factor for converting Curve I into Curve I' is thus simply the term $\frac{2 + \Delta X^o_c \; U^o_o}{2}$, by which the last term of equation (50) must be multiplied to yield the last term of equation (52). From this it is seen that the two approximation methods would be identical if U^o_o were zero, as in the case of no heat losses from the cloth surface; furthermore, the smaller the cloth increment, the smaller the conversion factor.

VI PRESENTATION AND DISCUSSION OF RESULTS

A. Analytical Results.

With the aid of the IBM 704 computer the complete "3-curve" solutions covering the following values of the independent variables have been determined;

$$\sqrt{\frac{(kc\rho)_s}{(kc\rho)_c}} = 5.0$$

$$U^o_i = 0.5,\ 1.0,\ 2.0,\ \text{and}\ 5.0$$

$$U^o_o = 0,\ 0.04,\ 0.1,\ \text{and}\ 0.2.$$

Each U_i^o value was matched successively with each U_o^o value for each of the three curves which represent energy absorption at different planes in the system having diathermanous cloth; thus 48 sets of calculations were required. The results are presented in Figures 12 to 26, inclusive, as plots of dimensionless temperature rise, ΔT^o vs. dimensionless time, $\Delta\theta_c^o$, with the third parameter on each curve being a particular combination of U_o^o and U_i^o. The curves extend up to 21.25 dimensionless time units and 1.05 dimensionless skin-depth units, which should make it possible with these data to solve problems of heat transfer through dry cloth to skin for radiation times ranging from 1 to 30 seconds.

Of the 15 final plots each of the first 14 represents the temperature rise at one of seven planes beneath the skin (or skin simulant) surface, for absorption of the radiant energy impulse at one of the first two arbitrarily chosen planes in the cloth-air-skin system. Because the curves for different combinations of U_o^o and U_i^o lie so close together some of them have not been drawn in but are instead represented by interpolation points. For Curve III the lines for various $U_o^o - U_i^o$ combinations for different planes are sufficiently separated to permit plotting the data for all seven skin-simulant planes on one sheet, which is Figure 26. The solution of any given problem, as described in Section V, is obtained by weighting the temperature-rise values given by the three curves, in accordance with the Beer-Lambert Law and the known diathermancy of the cloth.

The chief advantage of using the "3-curve method" in obtaining a general solution for any diathermanous cloth system is its simplicity. It is granted that better accuracy could be obtained if the general solution were made up by use of a larger number of curves, each of which would represent absorption of radiant energy in a particular increment. However, the small gain in accuracy would not justify the large increase in effort required, and the purpose of get-

ting a relatively simple general solution would be defeated.

Thus the justification of such a method depends almost entirely on the accuracy of the solution as against those calculated by the more complicated method discussed in Section IV. Test solutions have therefore been obtained, using the 6-slice model which was shown in Section III, above, to be close to the "true" solution.

The test consists of the following calculations:

(1) "Rigorous" solutions were obtained for two specific γL values. One corresponds to the low diathermancy, medium-grey cloth with $e^{-\gamma L}c = 6\%$, and one to the high diathermancy, white cloth with $e^{-\gamma L} = 42.8\%$. A 6-slice cloth model was used, and the procedure outlined in Section V was followed, assuming appropriate fractions of the radiation energy are absorbed in each of the six cloth slices and at the skin surface in accordance with the Beer-Lambert Law. The solution was carried out in 180 time increments corresponding to a dimensionless time value of 2.5.

(2) Solutions by the 3-curve method were then obtained, again using a six-slice model, with the radiation absorbed at the surface, at $X_c^o = 0.75$, and at the skin surface, respectively. Proper proportioning of these three curves gave the final solutions for the two types of cloth. (When $e^{-\gamma L} = .06$, the proportioning of the 3 curves is, I:II:III = 0.7555:0.185:0.06; and when $e^{-\gamma L} = .428$, I:II:III = .347:.225:.428.)

Results obtained by the two procedures are given in Tables IV and V for the cases of low and high diathermancy, respectively. It was not considered necessary to carry the solution beyond a dimensionless time of 2.50, since the percentage difference between the two results decreases with increasing time. It is evident from the tabulation that the use of the three-curve method is amply justified by the good results it gives.

B. Experimental Verification of Analytical Work.

If the physical and thermal properties of the cloth samples used in experiments were accurately known, comparison of experimental and theoretical results would be relatively straightforward. However, the properties are not all well known. As pointed out in Quarterly Status Report No. 14 of this program, literary values for thermal conductivity of cotton fabrics vary considerably and none are presently available for the 9-ounce cotton sateen samples which have been supplied by the Quartermaster R & D Command for the experimental work. Even if the conductivity values as usually determined were available, however, it is questionable that they could properly be applied for experiments involving radiant as well as conductive heat transmission. This difficulty arises from the non-homogeneity of cloth; the measured thickness used in the conventional conductivity determination would not be the proper effective thickness for a case involving radiation. Because of the ambiguity in the determination of an effective thickness, L_c, it has been found necessary to combine this property with other properties in the correlations. It is believed that the thermal conductance, k_c/L_c, should be the same for all six of the cotton sateen samples, regardless of their optical properties, and the comparison of experimental with theoretical data has become, in effect, a procedure for determining this property by trial and error.

Since the density of the cloth also depends upon how the thickness, L_c, is measured or defined, the specification of thickness has been avoided by use of the product $(\rho L)_c$, the value of which can be nicely determined under the same conditions as those prevailing when the cloth is used in thermal radiation experiments. To determine the density-thickness product duplicate samples were stretched over 5-inch embroidery rings and then cut out along the inside rim of the rings with a razor blade. The discs were then dried and weighed. The area

included by the rings (which are not perfect circles) was determined by measuring with a planimeter the area of paper samples similarly stretched over the rings and cut out. The $(\rho L)_c$ product so determined for four cloth samples (of different colors) was 0.0273 $\pm$ 2% gm/cm^2. Literature values for the heat capacity of cotton fabrics vary between about 0.32 (5) and 0.35 (1); a value of 0.335 cal/gm$^\circ$C has been used in this work. Thus the volumetric heat capacity $(c\rho L)_c$, of the cloth is between 0.0088 and 0.0095, or 0.0092 $\pm$ 8.7% cal/sq. cm$^\circ$C.

The physical and thermal properties of human skin are of course also variable. For the design of skin simulants used in experiments here the properties of average white skin agreed upon at an AFSWP conference (6) have been used. The agreed value for k_s is 1.065×10^{-3} cal/cm sec.$^\circ$C, and that of $(k\rho)_s$ is 8.5×10^{-4} cal^2/cm^4 sec $(^\circ C)^2$. While these values were used in its design, the performance of simulant No. 10 showed (by procedures previously reported (2), that for this simulant the actual k_s is 1.035×10^{-3} and $(k\rho)_s$ is 8.65×10^{-4}.

We consider next the heat transfer coefficients U_o and U_i for surface heat loss and for transmission through the gap between cloth and simulant, respectively. These appear in Figures 12 to 26 in the non-dimensional forms, $U_o^o = U_o L_c/k_c$ and $U_i^o = U_i L_c/k_c$. The value of U_o can be fairly well estimated from knowledge of heat transmission by natural convection. The value of U_i is more difficult to determine, especially for the experiments in which the cloth and skin simulant are in contact, so that the effective gap width is not measurable. In the procedure to be followed for comparing experimental and analytical results, (the determination of $(k/L)_c$ by trial), two courses are possible in the handling of these two heat transfer coefficients. The simpler way is to let U_o^o and U_i^o remain constant with each selection of $(k/L)_c$. Since this implies, unrealistically, that the coefficients U_o and U_i are variables, the more rigorous

procedure of keeping U_o and U_i fixed while letting U_o^o and U_i^o vary will be followed. This requires interpolation to new values on the T^o vs. θ_s^o charts with each new selection of $(k/L)_c$.

As an example of the procedure, a comparison will be made between experimental and theoretical temperature-time-depth data within skin simulant No. 10 upon its exposure to thermal radiation through an overlying and contacting layer of 9-ounce cotton sateen designated as light gray, or QM5. The intensity of test exposures ranged from 0.5 to 4.0 cal/sq.cm.sec. and the duration from 12 to 4 seconds. As measured by the Naval Material Laboratory (7), the transmittance, τ, and reflectance, R, determined by integration over the solar spectral range of 0.4μ to 2.4μ, were 7.4% and 56.0%, respectively, for the light gray sateen. Thus the fraction of unreflected radiant energy which passes through the back surface of the cloth, due to its diathermancy, is $e^{-\gamma L} = \tau/(1-R) = 0.1682$. This latter value requires that T^o values read from Figures 12 through 26 must be weighted in the ratio 0.5899:0.2419:0.1682 for Curve I, Curve II and Curve III data. While the T^o values can be read from the charts for any cloth-simulant systems, for the Q.M. cloth samples specifically, these values have been IBM-calculated with the weighting factors for diathermancy included. Copies of these tabulated data can be obtained by interested parties by arrangement with the M.I.T. Fuels Research Laboratory.

The simplest approach to comparing experimental and theoretical data is to make the first choice of $(k/L)_c$ be 1/266, the value which corresponds to a value of 5.0 for R, the square root of the ratio $(k\rho c)_s / (k\rho c)_c$. Having made this choice, the first step is to plot values of T^o vs. X_s^o for several values of dimensionless time, θ_s^o. The second step is to determine values of X_s^o corresponding to the thermocouple locations in Skin Simulant No. 10.

Since $X_s^o = \frac{x_s}{k_s} \cdot \frac{k_c}{L_c}$, this transformation is simply as tabulated below:

Thermocouple Number	x_s	$\frac{x_s}{k_s}$	$X_s^o = \frac{x_s}{k_s} \cdot \frac{1}{266}$
1	0.029 cm	28.0	0.1053
2	0.037	35.7	0.1342
4	0.068	65.7	0.2470
5	0.130	125.6	0.4720

For the X_s^o locations listed above, values of T^o are read and tabulated with the corresponding θ_s^o values.

The third step is to transform T^o and θ_s^o values into the form $\Delta T\, U_o/I_o$ and $\Delta\theta\, U_o^2/(kc\rho)_s$ which eliminates $(k/L)_c$. The transformation for temperature is simply:

$$\frac{\Delta T U_o}{I_o} = \frac{\Delta T K_c}{I_o L_c} \cdot \frac{U_o L_c}{k_c} = \frac{\Delta T^o U_o^o}{I_o};$$

and in our present example $\frac{\Delta T\, U_o^o}{I_o} = (0,1)\Delta T^o$.

The conversion for time is:

$$\frac{\Delta\theta\ U_o^2}{(kc\rho)_s} = \frac{\Delta\theta\, k_c}{(c\rho)_c L_c^2} \cdot \frac{(kc\rho)_c}{(kc\rho)_s} \cdot \left(\frac{U_o L_c}{k_c}\right)^2 = \theta_c^o \left(\frac{1}{R}\right)\left(U_o^o\right)^2,$$

which in this case is

$$\theta_c^o \left(\frac{1}{25}\right)\left(0.01\right) = 0.0004\theta_c^o$$

Step four of the procedure is to plot the new values of $\Delta TU_o/I_o$ vs. $\Delta\theta U_o^2/(kc\rho)_s$, for comparison with the experimental data. This comparison is conveniently made by plotting the experimental data as $\Delta T/I_o$, ^oC sq cm sec/cal, vs. θ, seconds, on a sheet of transparent vellum which can be laid over the

theoretical curves. Alignment of the two curves along the y-axis is made by matching $\Delta T/I_o$ equal to unity for the experimental data with the point where the theoretical $\Delta TU_o/I_o$ is equal to U_o, or $0.1/266 = 3.76 \times 10^{-4}$. Alignment along the x-axis is made by matching the experimental time of 1.0 second with the theoretical-data value of $U_o^2/(kc\rho)_s$, or $(3.76 \times 10^{-4})^2/8.65 \times 10^{-4} = 1.633 \times 10^{-4}$.

A plot of $\Delta T\, U_o/I_o$ vs. $\Delta\theta U_o^2/(kc\rho)_s$ is shown in Fig. 27, for the four thermocouples of Simulant No. 10. Superimposed on or near the curves are short vertical lines which represent the experimental data, the length of each of these lines indicating the estimated precision of the measurement. In order to test the assumption regarding $(k/L)_c$ and to determine how sensitive the correlation may be to this parameter, it is necessary to go through the procedure with another value of $(k/L)_c$.

For this second trial, $(k/L)_c$ is arbitrarily chosen as 1/240, consequently,

$$(kc\rho)_c = (c\rho L)_c \cdot \left(\frac{k}{L}\right)_c$$

$$= (0.0092 \pm 8.7\%)\left(\frac{1}{240}\right) = 3.836 \times 10^{-5} \pm 8.7\%,$$

and

$$R = \sqrt{(kc\rho)_s/(kc\rho)_c} = \sqrt{8.65 \times 10^{-4}/3.836 \times 10^{-5}}$$

$$= 4.75 \pm 2.95\%$$

Since the theoretical curves are based on R = 5.0, values of T^o read therefrom should be increased by a factor, $\left(\frac{5.0}{4.75}\right)^{0.89}$, which has been found empirically to be a satisfactory way to correlate calculations based on different "R" values. (This transformation makes it possible to use a single value of R for all theoretical curves, rather than a number of values, as are required for the parameters U_o^o and U_i^o.) Also from the new value of $(k/L)_c$, we find

$$U_o^o = 0.1 \frac{240}{266} = 0.0902$$

and $$U_i^o = 2.0 \frac{240}{266} = 1.802.$$

To make up a new plot of T^o vs. X_s^o, corresponding to these new heat transfer parameters, it is necessary to perform a double interpolation, using T^o data for U_o^o values of 0.04 and 0.10 and U_i^o values of 1.0 and 2.0. The 10% reduction in U_o^o makes a small upward change in T^o values for dimensionless times of 2.0 and more; for shorter times the effect is nearly negligible. The decrease in T^o caused by a 10% decrease in U_i^o is significant for all the dimensionless times of this example (i.e. to 6.0). Finally, the effect of the correction for change in the ratio R against increases T^o, so that the net effect of all three factors is an increase in T^o which is negligible for short time intervals and increasingly important for longer times.

The depth parameter, X_s^o, is also affected by changes in $(k/L)_c$ and the consequent change in R. Since

$$\frac{\Delta X_c^o}{\Delta X_s^o} = \sqrt{\frac{(kc\rho)_s}{(kc\rho)_c}} = R,$$

and ΔX_c^o is fixed at 0.5, a change of R from 5.0 to 4.75 causes ΔX_s^o to be changed to 0.1053. For this new case, therefore, the positions of planes F, G, H, etc. in the skin simulant are made deeper by the ratio, 0.1053/0.1. In other words, the dimensionless temperature values calculated and plotted for the case of R = 5, now apply for greater depths, because R = 4.75.

Again, the position of skin-simulant thermocouples in terms of X_s^o are also changed when $(k/L)_c$ is changed. The new depths are as follows:

Thermocouple	1	2	4	5
x_s/k_s	28.0	35.7	65.7	125.6
$X_s^o = \frac{x_s}{k_s} \frac{1}{240}$	0.1167	0.1487	0.274	0.523

The next step is to read values of T^o from the new T^o vs. X_s^o plot, tabulate them and make a conversion of the dimensionless time values to those from which $(k/L)_c$ is eliminated. The conversion this time is:

$$\frac{\Delta\theta\, U_o^2}{(kc\rho)_s} = \left(\frac{\Delta\theta\, k_c}{(c\rho)_c\, L_c^2}\right) \frac{(kc\rho)_c}{(kc\rho)_s} \left(\frac{U_o\, L_c}{k_c}\right)^2$$

$$= \theta_c^o \left(\frac{1}{R}\right)^2 \left(U_o^o\right)^2$$

$$= \left(\frac{1}{22.55}\right)\left(0.0081\right)\theta_c^o = 3.59 \times 10^{-4}\ \theta_c^o$$

Finally, a plot can be made of the theoretical data, corrected and converted as required by the choice of $(k/L)_c = 1/240$. The results are represented by the dashed-line curves of Figure 27. In the example chosen the dependence of results on $(k/L)_c$ is so small as to be barely perceptible when this parameter is changed by 10%. The reason that thermal conductance of the cloth is of so little importance is that a sizable fraction of the incident radiant energy passes through without dependence on conductance. Thus the temperature rise in skin behind a diathermanous cloth covering is rapid regardless of the conductance of the cloth. In this comparison of the experimental and theoretical data, the light gray cloth was chosen simply because the case of a diathermanous cloth is a more exacting test of the theoretical analysis. The comparison procedure is, of course, the same regardless of cloth type. The results shown in Figure 27 indicate that agreement between the experimental and theoretical work is remakably good. The agreement for relatively large values of dimensionless time, however, is not as good as desired, but could be improved by choice of a somewhat higher value for U_o. It is inevitable that a single comparison is not adequate for showing both (a) the applicability of the theory to cases involving use of diathermanouse cloth

and (b) a nice determination of $(k/L)_c$. Determination of $(k/L)_c$ was not the original purpose of this work. Rather the aim was simply to learn whether heat transfer in such a complex multi-component system could be adequately treated by theoretical analysis of a simplified model. This has been conclusively demonstrated, not only for opaque cloth systems but also for diathermanous cloth systems. In addition, application of the analysis to opaque cloth systems offers a good way of determining the effective value of thermal conductance of cloth $(k/L)_c$, when the heat source is radiant thermal energy. Results to date show that values of 1/260 to 1/270 are good for the cotton sateen samples.

VIII CONCLUSIONS

1. An analytical study has been made of heat transmission through dry cloth and air space to underlying skin, following exposure of the system to radiant thermal energy.

2. Both the simple case involving absorption of all the radiant energy at the radiated surface of opaque cloth and the more complicated case in which some of the energy is transmitted through diathermanous cloth can be satisfactorily solved numerically by finite-difference approximation.

3. For systems involving cloth of known diathermancy a technique which requires the use of only three curves, each representing absorption at a different plane in the system, gives results (in terms of temperature rise) within 1 to 2% of those obtained by machine computation for two specific cases wherein allowance was made for energy absorption at each of six slices in the cloth. These two cases represented cloths of very high and very low diathermancy, thus permitting the conclusion that use of the 3-curve method is a satisfactory substitute for machine computation of specific problems.

4. The curves necessary for solution of any problem involving heat transmission through dry cloth and an air space to skin have been determined by machine computation for the range of exposure times up to about 30 seconds.

5. Adequacy of the analysis and computation procedures have been verified by good agreement with the experimental results obtained by exposure of cloth-air-skin simulant systems to thermal radiation.

IX NOMENCLATURE

c	Heat capacity, cal/gm -^{o}C
I	Intensity of incident radiation, cal/cm^{2}-sec.
I_o	Intensity of unreflected radiation, cal/cm^{2}-sec.
k	Thermal conductivity, cal/cm-sec.-^{o}C
L	Thickness of cloth, cm
M	Modulus, $\left(X_c^o\right)^2 / \Delta\, \theta_c^o$
R	Ratio = $\Delta X_c^o / \Delta X_s^o = \sqrt{(kc\rho)_s / (kc\rho)_c}$
R	Reflectance of cloth
T	Temperature, ^{o}C
U	Overall heat transfer coefficient, cal/sq. cm.-sec.^{o}C
x, X	Depth, cm

Greek

γ	Extinction coefficient, cm^{-1}
Δ	Finite increment
θ	Time, sec.
ρ	Density, gm/cm^{3}
τ	Transmittance of cloth

Subscripts

c	Cloth
i	Air gap between cloth and skin simulant
o	Cloth surface
s	Skin simulant
A, B, ... n, n+1	Depth planes
0, 1.... m, m+1	Time increments

Superscript

o	Dimensionless group.

IX. REFERENCES

(1) Ho Leong, B. and Williams, M.E.: "Surface Temperatures in a Two-Layer Air-Spaced Slab System Irradiated from One Side"; Technical Rept. No. 4, D.I.C. Project 6797, Fuels Research Laboratory, M.I.T., Cambridge, Mass., Jan. 30, 1956.

(2) Chen, N.Y. and Jensen, W.P.: "Skin Simulants with Depth Magnification", Tech. Rpt. No. 5, DSR Project 7666, Fuels Research Laboratory, M.I.T., Cambridge, Mass., March 15, 1957.

(3) McAdams, W.H.: "Heat Transmission", Ch. III, 3rd ed., New York, McGraw-Hill Book Co., Inc., 1954

(4) Gardon, R.: "Temperature Attained in Wood Exposed to High Intensity Thermal Radiation"; Tech. Rpt. No. 3, D.I.C. Project 6797, Fuels Research Laboratory, M.I.T., Cambridge, Mass., 1953.

(5) Dietz: Leipzig Monatsch Textile (1912); quoted in "International Critical Tables", Vol. II, p. 237, New York, McGraw-Hill Book Co., Inc. (1927).

(6) AFSWP Conference at Technical Operations, Inc., Arlington, Mass., 1955.

(7) Naval Material Laboratory: "Research Report on the Spectral Reflectance and Transmittance of Standard Fabrics for Thermal Radiation Effects Studies", Lab. Project 5046-3, Part 91, August 1956.

TABLE I.

COMPARISON OF 6-SLICE MODEL WITH 2-SLICE MODEL

TEMPERATURE PROFILE IN OPAQUE CLOTH

X_c^o / $\Delta\Theta_c^o$ / ΔT^o	-1/4			+1/4			3/4			1 1/4		
	2-slice	6-slice	% diff.	2-slice	6-slice	% diff.	2-slice	6-slice	% diff.	2-slice	6-slice	% diff.
.2500	.8566	-		.3688	.3493	+ 5.6	.1238	.1202	+ 3.0	.0969	-	-
.5000	1.0873	-		.6042	.5898	+ 2.4	.3365	.3256	+ 3.3	.2647	-	-
.7500	1.2926	-		.8136	.7994	+ 1.8	.5271	.5153	+ 2.3	.4161	-	-
1.000	1.4761	-		1.0009	.9865	+ 1.5	.6979	.6859	+ 1.8	.5524	-	-
1.250	1.6405	-		1.1686	1.1543	+ 1.2	.8512	.8391	+ 2.4	.6753	-	-
1.500	1.7880	-		1.3191	1.3051	+ 1.1	.9890	.9770	+ 1.2	.7863	-	-
1.7500	1.9206	-		1.4544	1.4407	+ 0.9	1.1131	1.1013	+ 1.1	.8867	-	-
2.0000	2.0401	-		1.5762	1.5629	+ 0.8	1.2251	1.2135	+ 1.0	.9776	-	-
2.2500	2.1478	-		1.6861	1.6733	+ 0.8	1.3262	1.3150	+ 0.9	1.0602	-	-
2.5000	2.2451	2.2335*	+ 0.5	1.7854	1.7731	+ 0.7	1.4178	1.4070	+ 0.8	1.1352	1.1271*	0.7

Note: R = 5.0 ΔX_c^o = 1/2 and 1/6

U_o^o = .04 * extrapolated value

U_i^o = 0.5

TABLE II.

COMPARISON OF 6-SLICE MODEL WITH 2-SLICE MODEL: TEMPERATURE PROFILE INSIDE SKIN SIMULANT

X_s^o / $\Delta\theta_c^o$	.05			.15			.25			.35			.55		
	2 slice	6 slice	% diff.	2 slice	6 slice	% diff.	2 slice	6 slice	% diff.	2 slice	6 slice	% diff.	2 slice	6 slice	% diff.
.2500	0	.0009	-	0	.0001	-	0	0	-	0	0	-	0	0	-
.5000	.0063	.0068	- 7.4	.0013	.0019	-31.6	0	.0004	-	0	.0001	-	0	0	-
.7500	.0163	.0164	- 0.6	.0058	.0063	- 7.9	.0016	.0021	-23.8	.0003	.0006	-50.0	0	0	-
1.000	.0283	.0283	0	.0126	.0130	- 3.1	.0049	.0054	- 9.3	.0016	.0020	-20.0	.0001	.0002	-50.0
1.2500	.0417	.0416	+ 0.2	.0211	.0213	- 0.9	.0096	.0101	- 4.9	.0040	.0045	-11.1	.0004	.0007	-42.9
1.5000	.0565	.0559	+ 1.1	.0309	.0309	- 0	.0157	.0161	- 2.5	.0074	.0079	- 6.3	.0012	.0015	-20.0
1.7500	.0715	.0708	+ 1.0	.0415	.0414	+ 0.2	.0227	.0231	- 1.7	.0117	.0122	- 4.1	.0025	.0029	-13.8
2.000	.0869	.0861	+ 0.9	.0529	.0527	+ 0.4	.0306	.0309	- 1.0	.0169	.0173	- 2.3	.0043	.0047	- 8.5
2.2500	.1024	.1015	+ 0.9	.0647	.0644	+ 0.5	.0392	.0393	- 0.3	.0227	.0231	- 1.7	.0066	.0070	- 5.7
2.5000	.1179	.1170	+ 0.8	.0770	.0765	+ 0.7	.0483	.0483	0	.0292	.0295	- 1.0	.0093	.0098	- 5.1

Note: Numbers in body of table indicate T^o

TABLE III.

COMPARISON OF MODIFIED AND ORIGINAL SCHMIDT METHODS WITH ANALYTICAL SOLUTION FOR HEAT TRANSMISSION IN A SEMI-INFINITE OPAQUE SOLID IRRADIATED ON ONE SIDE

ΔX_c^o / $\Delta\theta_c^o$ ΔT^o	-1/9			1/9			3/9			5/9			7/9			1.0		
	M.S.	Sch.	Ana.	M.S.	Sch.	Ana.	M.S.	Sch.	Ana.	M.S.	Sch.	Ana.	M.S.	Sch.	Ana.	M.S.	Sch.	Ana.
0																		
.0247																		
.0494													0	0	.0011	0	0	.0001
.0741										.0275	.0139	.0247	0	0	.0065			
.0988							.1224	.0776	.1120	.0409	.0242	.0420						
.1235				.2968	.2141	.2800	.1490	.1009	.1430									
.1481	.5421	.4256	.5466*	.3295	.2456	.3220												

Notes: M.S. = Modified Schmidt; Sch = Schmidt Method; Ana = Analytical

$U_o^o = 0.1$, $\Delta X_c^o = 1/9$, $\Delta\theta_c^o = .02469$

* extrapolated value

TABLE IV.

DIMENSIONLESS TEMPERATURE RISE IN LOW-DIATHERMANCY CLOTH ($e^{-\gamma L} = 0.06$) AND UNDERLYING SKIN: COMPARISON OF SIX-SLICE "EXACT" AND "THREE-CURVE" SOLUTIONS.

$U_o^o = 0.04$, $U_i^o = 0.5$, $R = 5.0$

	$X_c^o = 0.25$		$X_c^o = 0.75$		$X_s^o = 0.05$		0.15		0.25	
$\Delta\theta_c^o$	Exact	3-curve	Exact	3-curve	Exact	3-curve	Exact	3-curve	Exact	3-curve
0.	0.	0.	0.	0.	0.	0.	0.	0.	0.	0.
0.1250	0.1584	0.1635	0.0664	0.0675	0.0027	0.0027	0.0004	0.0004	0.0000	0.0000
0.2500	0.2905	0.2912	0.1575	0.1630	0.0059	0.0060	0.0015	0.0015	0.0003	0.0003
0.3750	0.4047	0.4047	0.2555	0.2614	0.0099	0.0103	0.0032	0.0033	0.0009	0.0009
0.5000	0.5109	0.5104	0.3503	0.3563	0.0148	0.0153	0.0056	0.0058	0.0018	0.0019
0.6250	0.6106	0.6099	0.4408	0.4467	0.0203	0.0209	0.0085	0.0087	0.0032	0.0033
0.7500	0.7049	0.7040	0.5266	0.5324	0.0264	0.0271	0.0119	0.0122	0.0049	0.0050
0.8750	0.7941	0.7931	0.6080	0.6136	0.0328	0.0336	0.0158	0.0162	0.0069	0.0071
1.0000	0.8786	0.8774	0.6852	0.6907	0.0396	0.0404	0.0200	0.0205	0.0094	0.0096
1.1250	0.9587	0.9574	0.7584	0.7638	0.0467	0.0475	0.0246	0.0251	0.0121	0.0124
1.2500	1.0346	1.0332	0.8278	0.8331	0.0539	0.0548	0.0295	0.0300	0.0152	0.0155
1.3750	1.1066	1.1050	0.8937	0.8990	0.0613	0.0623	0.0346	0.0352	0.0185	0.0188
1.5000	1.1749	1.1733	0.9563	0.9615	0.0689	0.0699	0.0400	0.0406	0.0220	0.0224
1.6250	1.2397	1.2380	1.0158	1.0209	0.0765	0.0776	0.0455	0.0462	0.0258	0.0262
1.7500	1.3013	1.2995	1.0723	1.0773	0.0842	0.0854	0.0512	0.0520	0.0298	0.0303
1.8750	1.3598	1.3579	1.1261	1.1310	0.0920	0.0932	0.0570	0.0578	0.0339	0.0344
2.0000	1.4153	1.4134	1.1772	1.1821	0.0998	0.1010	0.0630	0.0638	0.0382	0.0388
2.1250	1.4682	1.4662	1.2259	1.2307	0.1076	0.1089	0.0690	0.0699	0.0427	0.0433
2.2500	1.5185	1.5164	1.2722	1.2770	0.1155	0.1167	0.0752	0.0761	0.0472	0.0479
2.3750	1.5663	1.5642	1.3163	1.3211	0.1233	0.1246	0.0814	0.0823	0.0519	0.0526
2.5000	1.6118	1.6097	1.3583	1.3631	0.1311	0.1324	0.0876	0.0886	0.0567	0.0574

	$X_s^o = 0.35$		0.45		0.55		0.65	
θ_c^o	Exact	3-curve	Exact	3-curve	Exact	3-curve	Exact	3-curve
0.	0.	0.	0.	0.	0.	0.	0.	0.
0.1250	0.	0.	0.	0.	0.	0.	0.	0.
0.2500	0.0000	0.0000	0.0000	0.	0.	0.	0.	0.
0.3750	0.0002	0.0002	0.0000	0.0000	0.0000	0.0000	0.0000	0.
0.5000	0.0005	0.0005	0.0001	0.0001	0.0000	0.0000	0.0000	0.
0.6250	0.0010	0.0011	0.0003	0.0003	0.0001	0.0001	0.0000	0.0000
0.7500	0.0018	0.0018	0.0006	0.0006	0.0002	0.0002	0.0000	0.0000
0.8750	0.0028	0.0029	0.0010	0.0011	0.0003	0.0003	0.0001	0.0001
1.0000	0.0041	0.0042	0.0016	0.0017	0.0006	0.0006	0.0002	0.0002
1.1250	0.0056	0.0057	0.0024	0.0024	0.0009	0.0010	0.0003	0.0003
1.2500	0.0073	0.0075	0.0033	0.0034	0.0014	0.0014	0.0005	0.0006
1.3750	0.0093	0.0095	0.0044	0.0045	0.0020	0.0020	0.0008	0.0008
1.5000	0.0115	0.0117	0.0057	0.0058	0.0026	0.0027	0.0012	0.0012
1.6250	0.0139	0.0142	0.0071	0.0073	0.0035	0.0035	0.0016	0.0016
1.7500	0.0165	0.0168	0.0087	0.0089	0.0044	0.0045	0.0021	0.0021
1.8750	0.0193	0.0196	0.0105	0.0107	0.0055	0.0056	0.0027	0.0028
2.0000	0.0222	0.0226	0.0124	0.0126	0.0066	0.0068	0.0034	0.0035
2.1250	0.0254	0.0258	0.0145	0.0147	0.0079	0.0081	0.0042	0.0043
2.2500	0.0286	0.0290	0.0167	0.0170	0.0094	0.0095	0.0050	0.0051
2.3750	0.0320	0.0325	0.0190	0.0193	0.0109	0.0111	0.0060	0.0061
2.5000	0.0355	0.0360	0.0215	0.0218	0.0126	0.0128	0.0071	0.0072

TABLE V.

DIMENSIONLESS TEMPERATURE RISE IN HIGH-DIATHERMANCY CLOTH ($e^{-\gamma L} = 0.428$) AND UNDERLYING SKIN: COMPARISON OF SIX-SLICE "EXACT" AND "THREE-CURVE" SOLUTIONS.

$U_o^o = 0.04$, $U_i^o = 0.5$, $R = 5.0$

	$X_c^o = 0.25$		$X_c^o = 0.75$		$X_s^o = 0.05$		0.15		0.25	
$\Delta\theta_c^o$	Exact	3-curve	Exact	3-curve	Exact	3-curve	Exact	3-curve	Exact	3-curve
0.	0.	0.	0.	0.	0.	0.	0.	0.	0.	0.
0.1250	0.0793	0.0814	0.0651	0.0612	0.0172	0.0172	0.0025	0.0025	0.0001	0.0001
0.2500	0.1552	0.1543	0.1267	0.1256	0.0308	0.0310	0.0090	0.0091	0.0018	0.0018
0.3750	0.2241	0.2228	0.1893	0.1882	0.0424	0.0427	0.0164	0.0165	0.0049	0.0050
0.5000	0.2895	0.2878	0.2492	0.2482	0.0532	0.0536	0.0237	0.0239	0.0089	0.0090
0.6250	0.3515	0.3497	0.3065	0.3053	0.0634	0.0639	0.0311	0.0313	0.0133	0.0134
0.7500	0.4106	0.4086	0.3610	0.3597	0.0732	0.0738	0.0383	0.0386	0.0181	0.0182
0.8750	0.4669	0.4648	0.4130	0.4115	0.0828	0.0834	0.0456	0.0460	0.0230	0.0232
1.0000	0.5205	0.5182	0.4625	0.4609	0.0922	0.0928	0.0529	0.0533	0.0281	0.0283
1.1250	0.5716	0.5692	0.5097	0.5080	0.1013	0.1021	0.0601	0.0606	0.0333	0.0336
1.2500	0.6203	0.6177	0.5547	0.5529	0.1104	0.1112	0.0673	0.0678	0.0387	0.0390
1.3750	0.6667	0.6640	0.5977	0.5958	0.1193	0.1201	0.0745	0.0751	0.0441	0.0444
1.5000	0.7109	0.7081	0.6387	0.6367	0.1281	0.1290	0.0817	0.0823	0.0496	0.0499
1.6250	0.7531	0.7502	0.6778	0.6757	0.1368	0.1377	0.0889	0.0894	0.0551	0.0555
1.7500	0.7934	0.7904	0.7151	0.7130	0.1454	0.1463	0.0960	0.0966	0.0607	0.0611
1.8750	0.8318	0.8288	0.7508	0.7486	0.1539	0.1548	0.1031	0.1037	0.0664	0.0668
2.0000	0.8685	0.8654	0.7849	0.7827	0.1623	0.1632	0.1101	0.1108	0.0720	0.0725
2.1250	0.9036	0.9004	0.8176	0.8152	0.1706	0.1716	0.1172	0.1179	0.0777	0.0782
2.2500	0.9371	0.9339	0.8488	0.8464	0.1788	0.1798	0.1241	0.1249	0.0834	0.0839
2.3750	0.9692	0.9659	0.8786	0.8762	0.1869	0.1879	0.1311	0.1318	0.0892	0.0897
2.5000	0.9998	0.9965	0.9072	0.9047	0.1949	0.1959	0.1380	0.1388	0.0949	0.0955

	0.35		0.45		0.55		0.65	
θ_c^o	Exact	3-curve	Exact	3-curve	Exact	3-curve	Exact	3-curve
0.	0.	0	0.	0.	0.	0.	0.	0.
0.1250	0.	0	0.	0.	0.	0.	0.	0.
0.2500	0.0002	0.0002	0.0000	0.0000	0.	0.	0.	0.
0.3750	0.0011	0.0011	0.0002	0.0002	0.0000	0.0000	0.0000	0.
0.5000	0.0027	0.0028	0.0007	0.0007	0.0001	0.0001	0.0000	0.0000
0.6250	0.0050	0.0050	0.0015	0.0016	0.0004	0.0004	0.0001	0.0001
0.7500	0.0075	0.0076	0.0028	0.0028	0.0009	0.0009	0.0002	0.0002
0.8750	0.0105	0.0106	0.0043	0.0043	0.0016	0.0016	0.0005	0.0005
1.0000	0.0137	0.0138	0.0061	0.0062	0.0025	0.0025	0.0009	0.0009
1.1250	0.0172	0.0173	0.0082	0.0082	0.0036	0.0036	0.0014	0.0014
1.2500	0.0208	0.0209	0.0104	0.0105	0.0048	0.0049	0.0021	0.0021
1.3750	0.0246	0.0248	0.0129	0.0130	0.0063	0.0064	0.0029	0.0029
1.5000	0.0285	0.0287	0.0155	0.0156	0.0079	0.0080	0.0038	0.0038
1.6250	0.0326	0.0328	0.0183	0.0184	0.0097	0.0098	0.0048	0.0049
1.7500	0.0367	0.0370	0.0212	0.0213	0.0116	0.0117	0.0060	0.0061
1.8750	0.0410	0.0413	0.0242	0.0244	0.0136	0.0137	0.0073	0.0074
2.0000	0.0453	0.0456	0.0273	0.0275	0.0158	0.0159	0.0087	0.0088
2.1250	0.0497	0.0500	0.0306	0.0308	0.0181	0.0182	0.0102	0.0103
2.2500	0.0542	0.0545	0.0339	0.0341	0.0204	0.0206	0.0118	0.0119
2.3750	0.0587	0.0591	0.0373	0.0376	0.0229	0.0230	0.0135	0.0136
2.5000	0.0632	0.0636	0.0408	0.0411	0.0254	0.0256	0.0153	0.0154

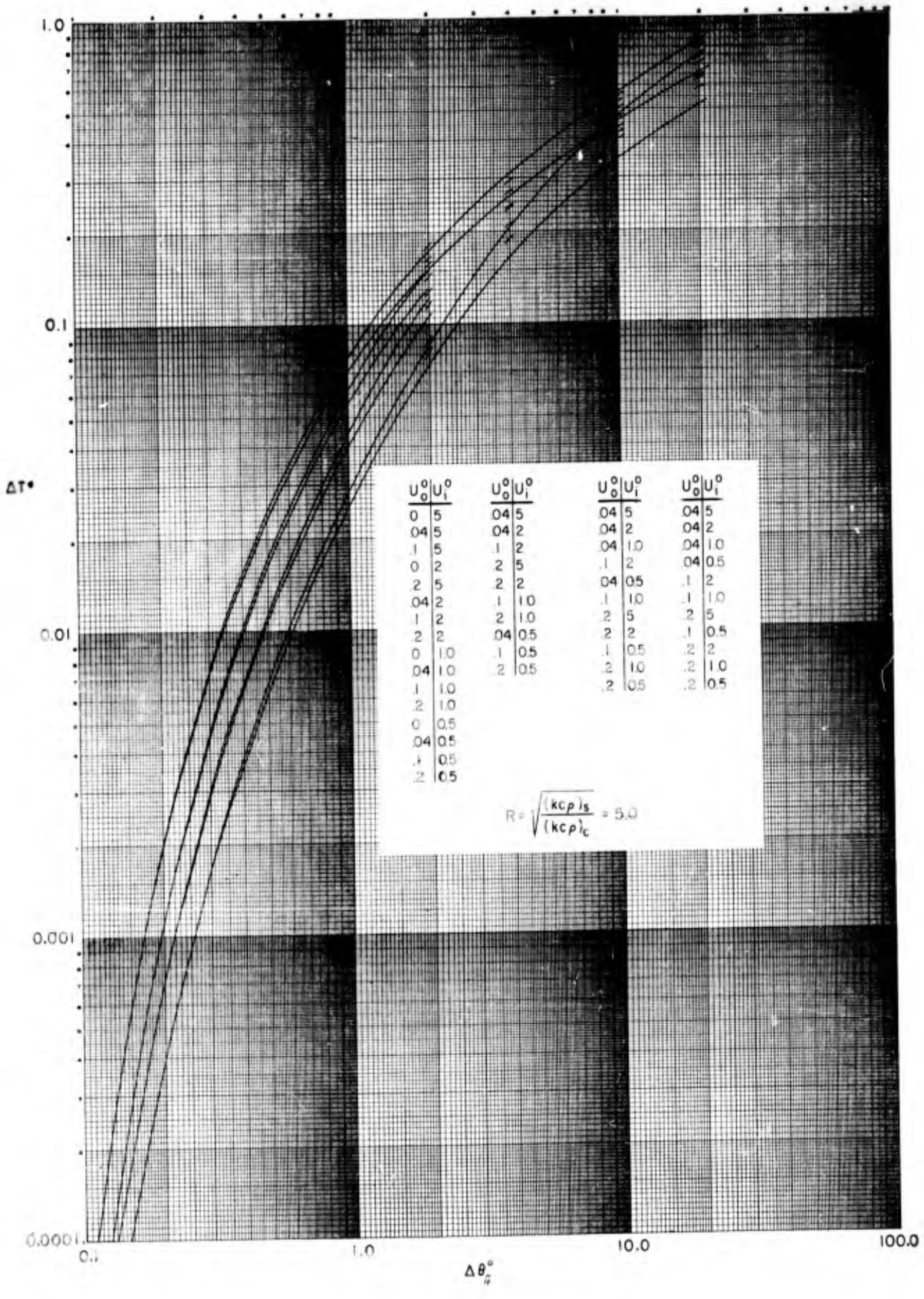

FIG. 12 - TEMPERATURE HISTORY WITHIN AN OPAQUE SEMI-INFINITE SOLID (SKIN) FOLLOWING THERMAL IRRADIATION THROUGH AN OVERLYING CLOTH LAYER. $X_S^o = 0.05$
(Curve I - All radiation absorbed at $X_C^o = 0$)

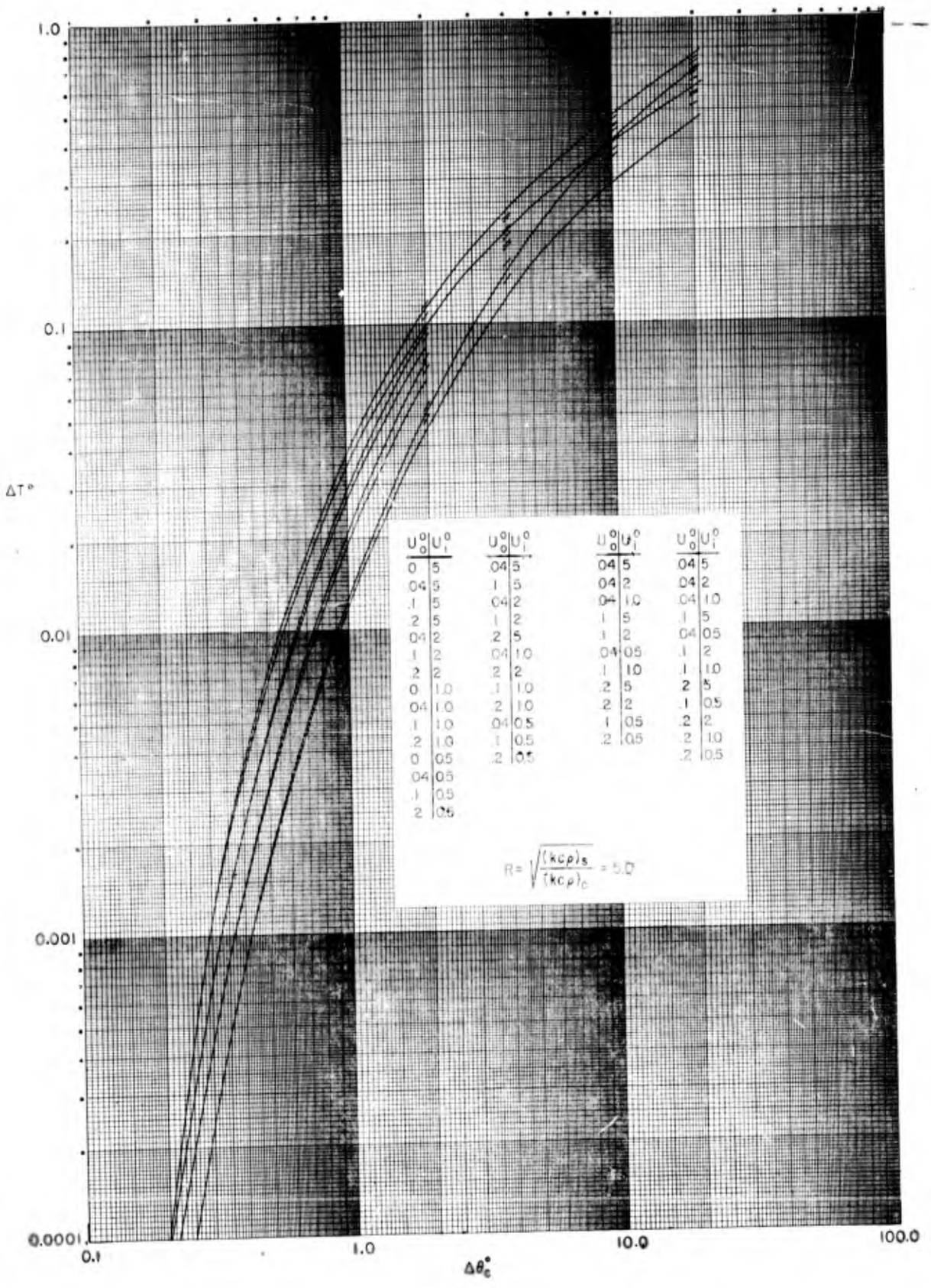

FIG. 13 - TEMPERATURE HISTORY WITHIN AN OPAQUE SEMI-INFINITE SOLID (SKIN) FOLLOWING THERMAL IRRADIATION THROUGH AN OVERLYING CLOTH LAYER. $X_s^o = 0.15$
(Curve I - All radiation absorbed at $X_c^o = 0$)

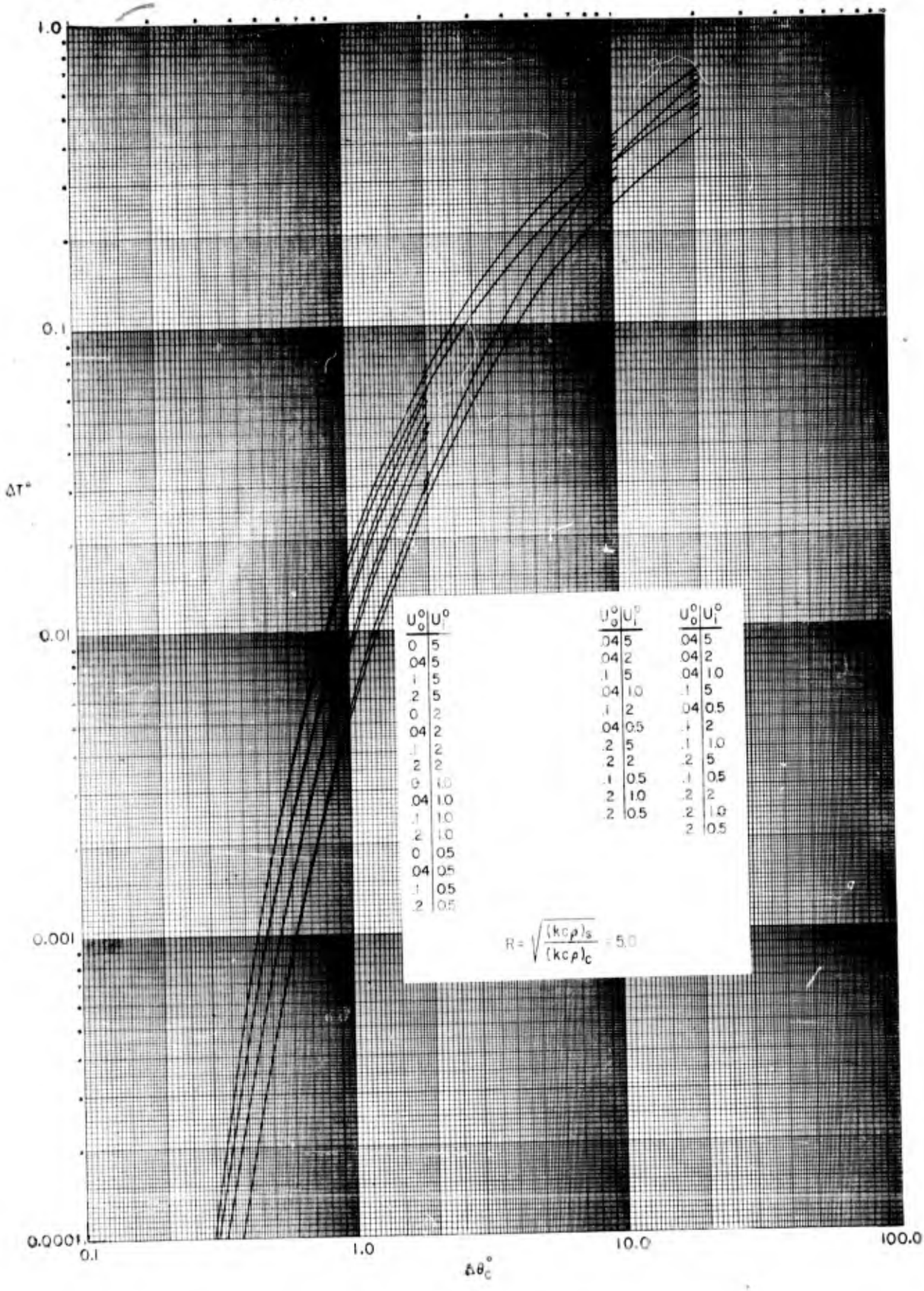

FIG. 14 - TEMPERATURE HISTORY WITHIN AN OPAQUE SEMI-INFINITE SOLID (SKIN) FOLLOWING THERMAL IRRADIATION THROUGH AN OVERLYING CLOTH LAYER. $X_s^o = 0.25$
(Curve I- All radiation absorbed at $X_c^o = 0$)

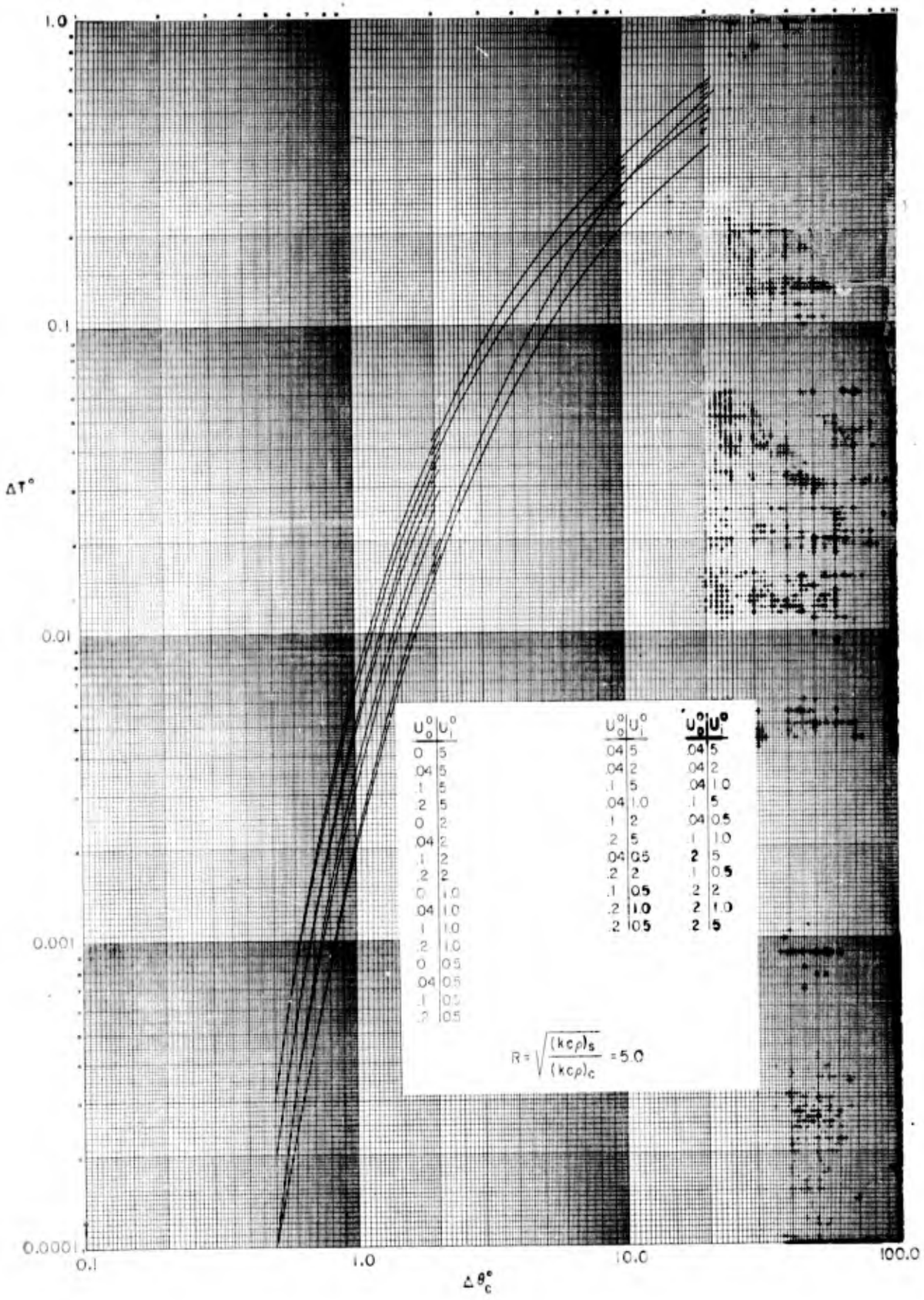

FIG. 15 - TEMPERATURE HISTORY WITHIN AN OPAQUE SEMI-INFINITE SOLID (SKIN) FOLLOWING THERMAL IRRADIATION THROUGH AN OVERLYING CLOTH LAYER. $X_S^0 = 0.35$
(Curve I – All radiation absorbed at $X_C^0 = 0$

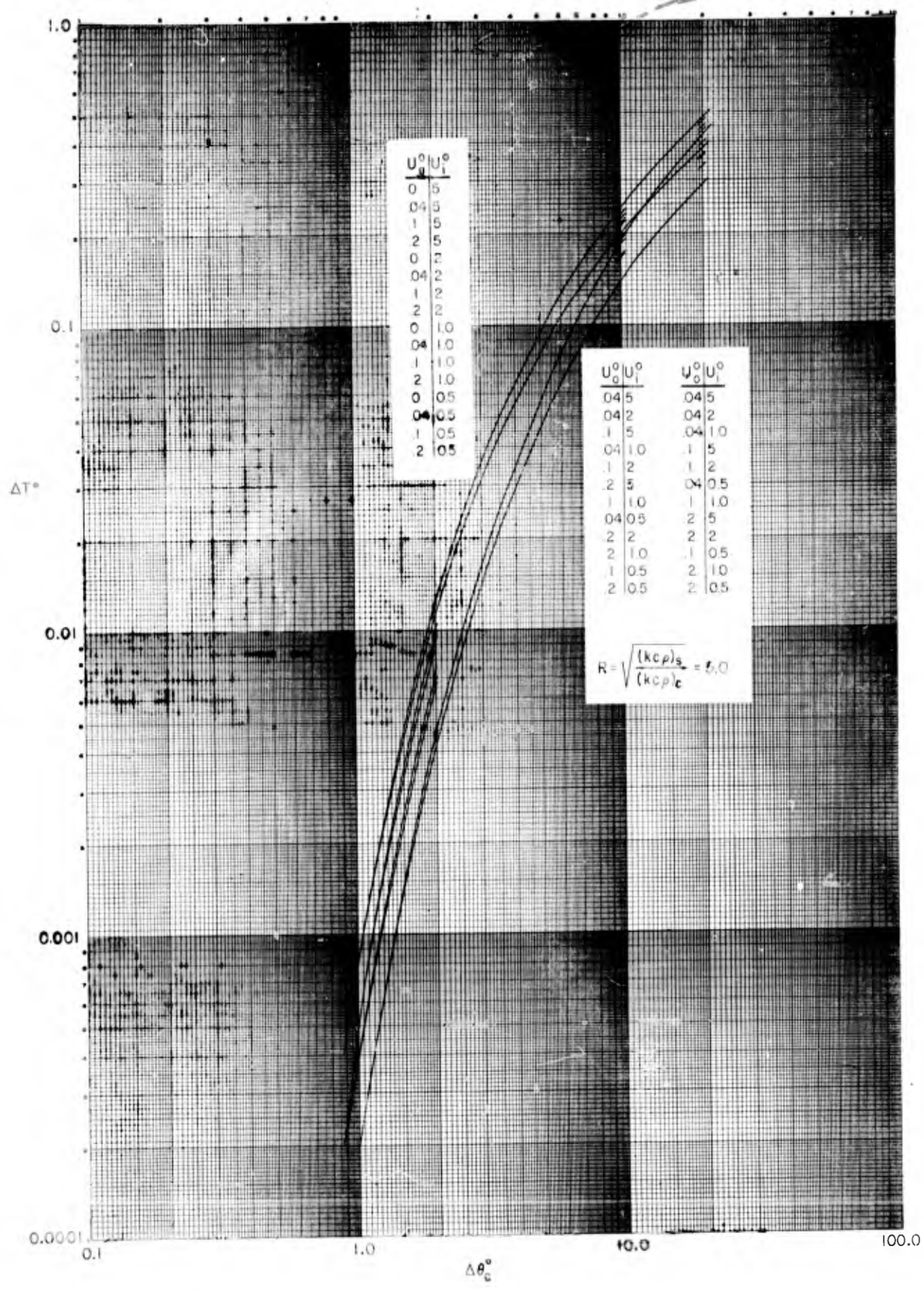

FIG. 16 - TEMPERATURE HISTORY WITHIN AN OPAQUE SEMI-INFINITE SOLID (SKIN) FOLLOWING THERMAL IRRADIATION THROUGH AN OVERLYING CLOTH LAYER. $X_s^o = 0.55$
(Curve I - All radiation absorbed at $X_c^o = 0$)

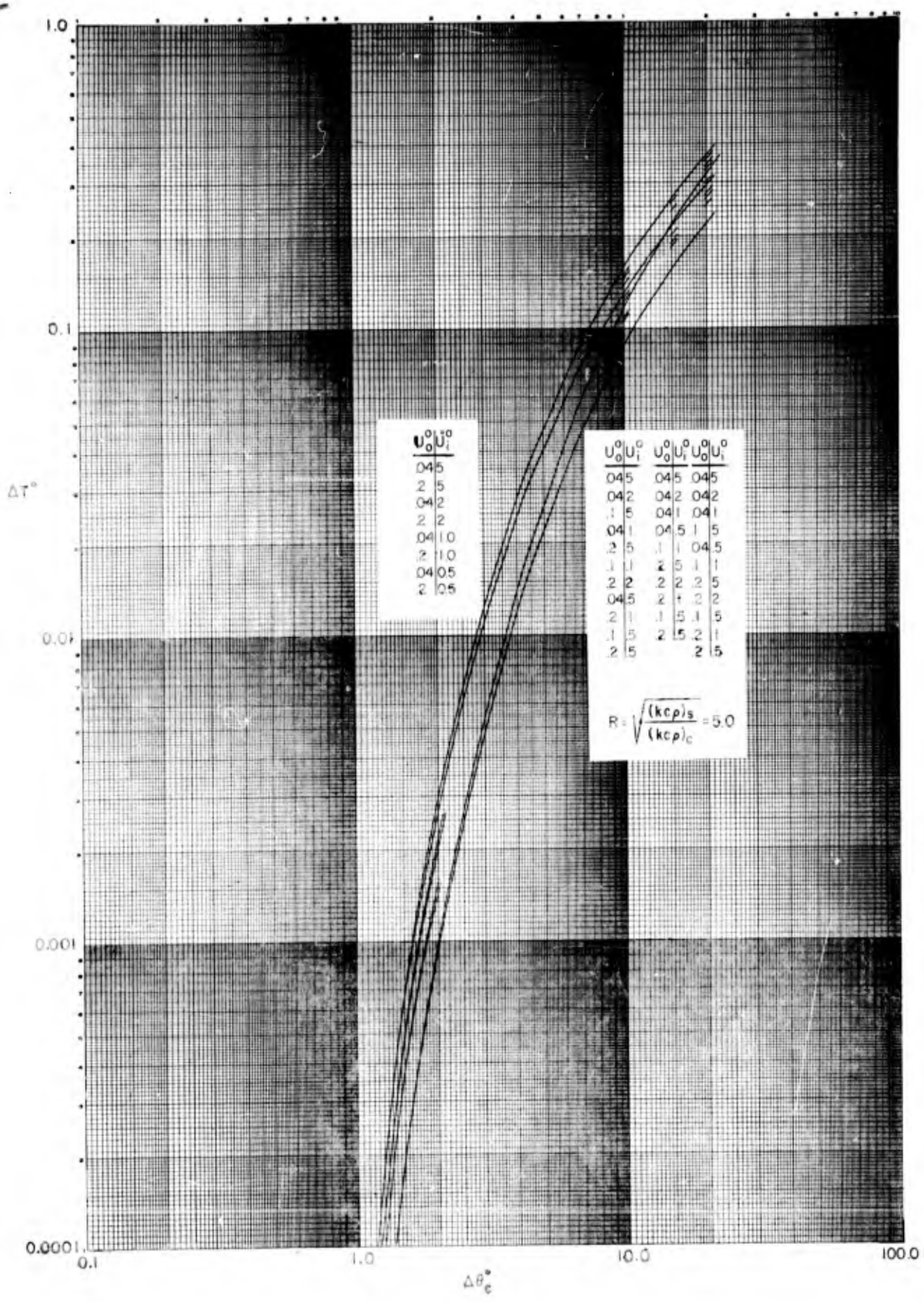

FIG. 17 - TEMPERATURE HISTORY WITHIN AN OPAQUE SEMI-INFINITE SOLID (SKIN) FOLLOWING THERMAL IRRADIATION THROUGH AN OVERLYING CLOTH LAYER. $X^{\circ}_{s} = 0.75$
(Curve I - All radiation absorbed at $X^{\circ}_{c} = 0$)

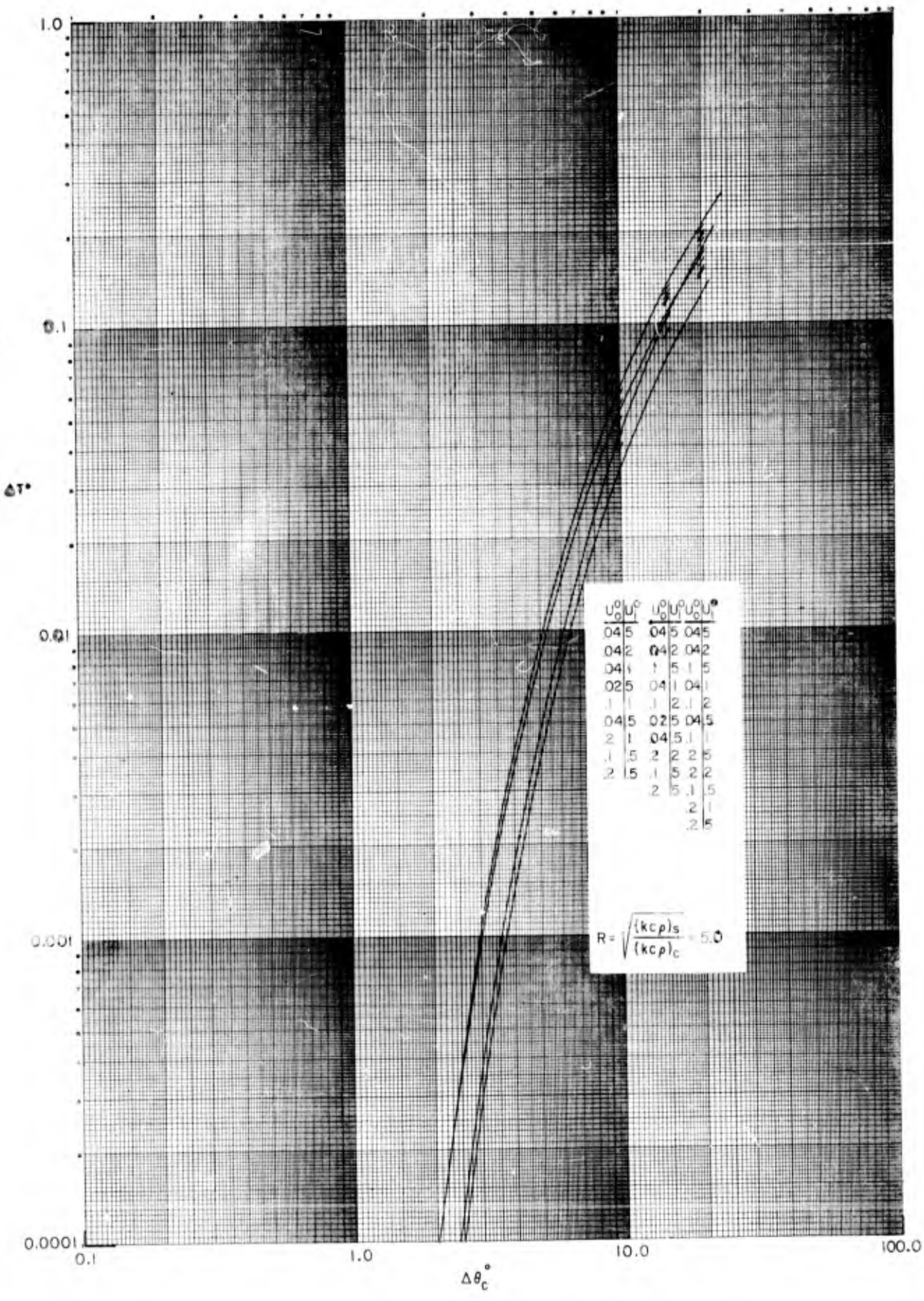

FIG. 18- TEMPERATURE HISTORY WITHIN AN OPAQUE SEMI-INFINITE SOLID (SKIN) FOLLOWING THERMAL IRRADIATION THROUGH AN OVERLYING CLOTH LAYER. $X_s^o = 1.05$
(Curve I- All radiation absorbed at $X_c^o = 0$)

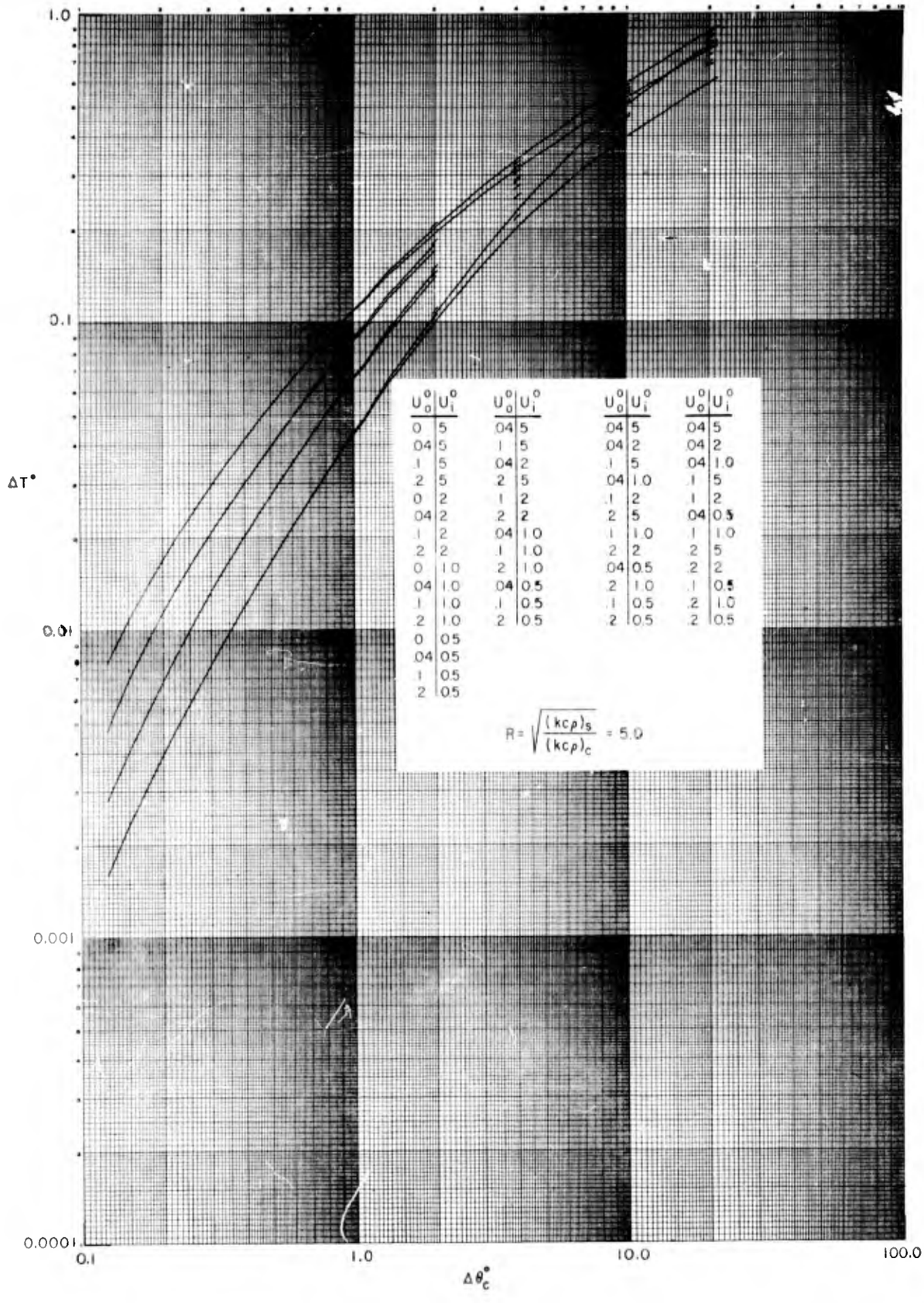

FIG. 19 - TEMPERATURE HISTORY WITHIN AN OPAQUE SEMI-INFINITE SOLID (SKIN) FOLLOWING THERMAL IRRADIATION THROUGH AN OVERLYING CLOTH LAYER. $X_s^o = 0.05$
(Curve II – All radiation absorbed at $X_c^o = 0.75$)

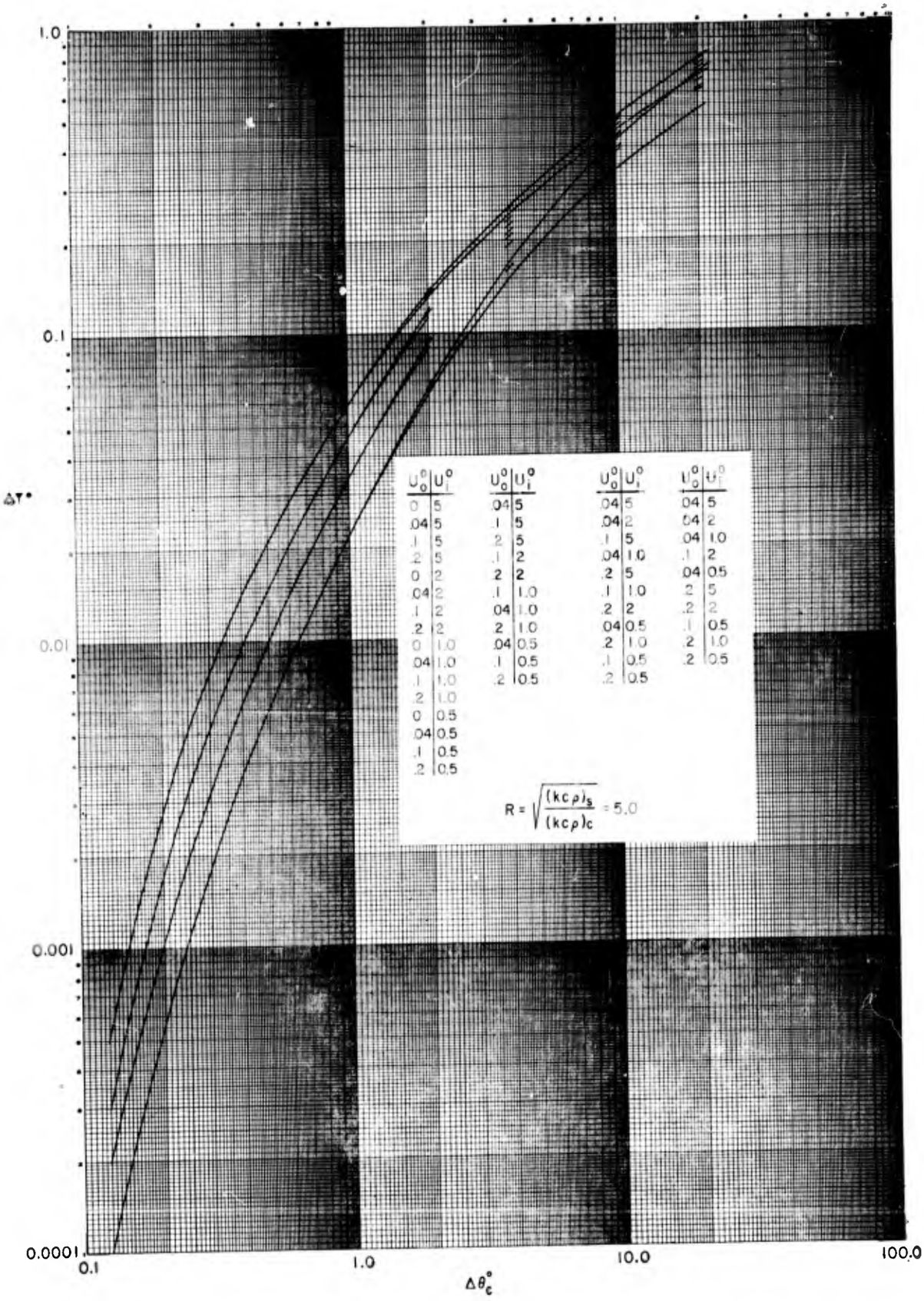

FIG.20 – TEMPERATURE HISTORY WITHIN AN OPAQUE SEMI-INFINITE SOLID (SKIN) FOLLOWING THERMAL IRRADIATION THROUGH AN OVERLYING CLOTH LAYER. $X^{\circ}_{s} = 0.15$
(Curve II – All radiation absorbed at $X^{\circ}_{c} = 0.75$)

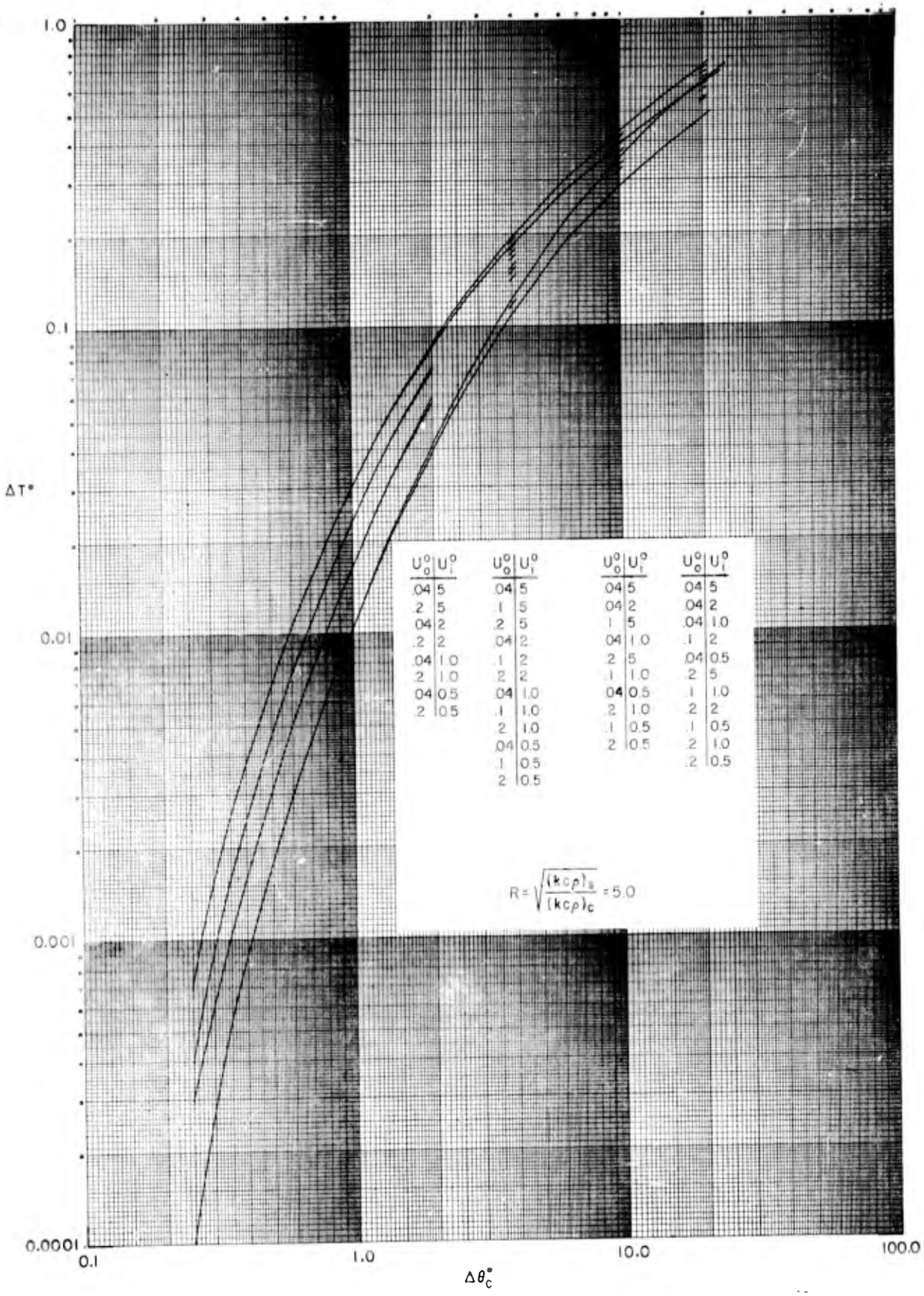

FIG.21 – TEMPERATURE HISTORY WITHIN AN OPAQUE SEMI-INFINITE SOLID (SKIN) FOLLOWING THERMAL IRRADIATION THROUGH AN OVERLYING CLOTH LAYER. $X_S^o = 0.25$
(Curve II – All radiation absorbed at $X_C^o = 0.75$)

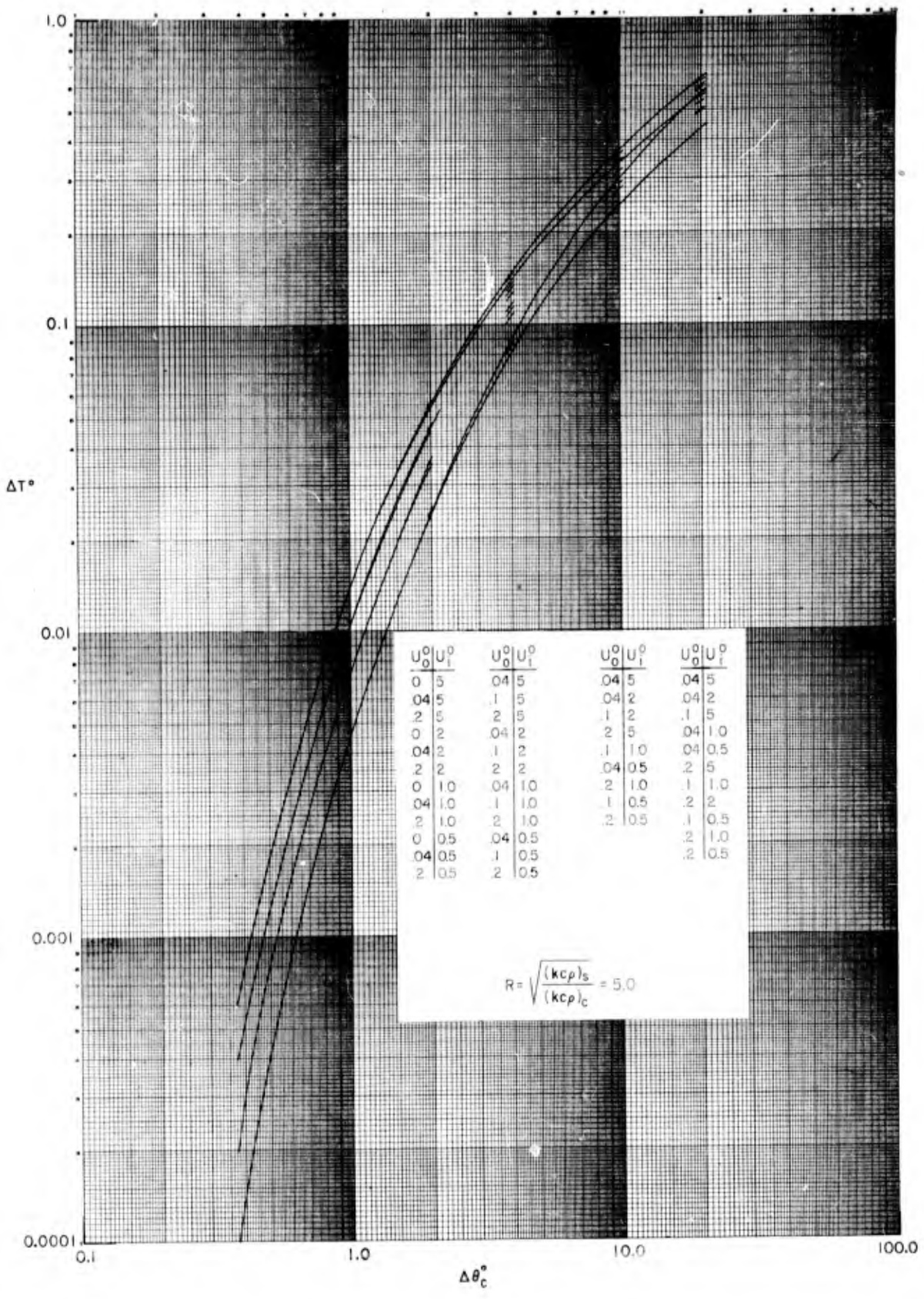

FIG.22- TEMPERATURE HISTORY WITHIN AN OPAQUE SEMI-INFINITE SOLID (SKIN) FOLLOWING THERMAL IRRADIATION THROUGH AN OVERLYING CLOTH LAYER. $X_s^0 = 0.35$
(Curve II - All radiation absorbed at $X_c^0 = 0.75$)

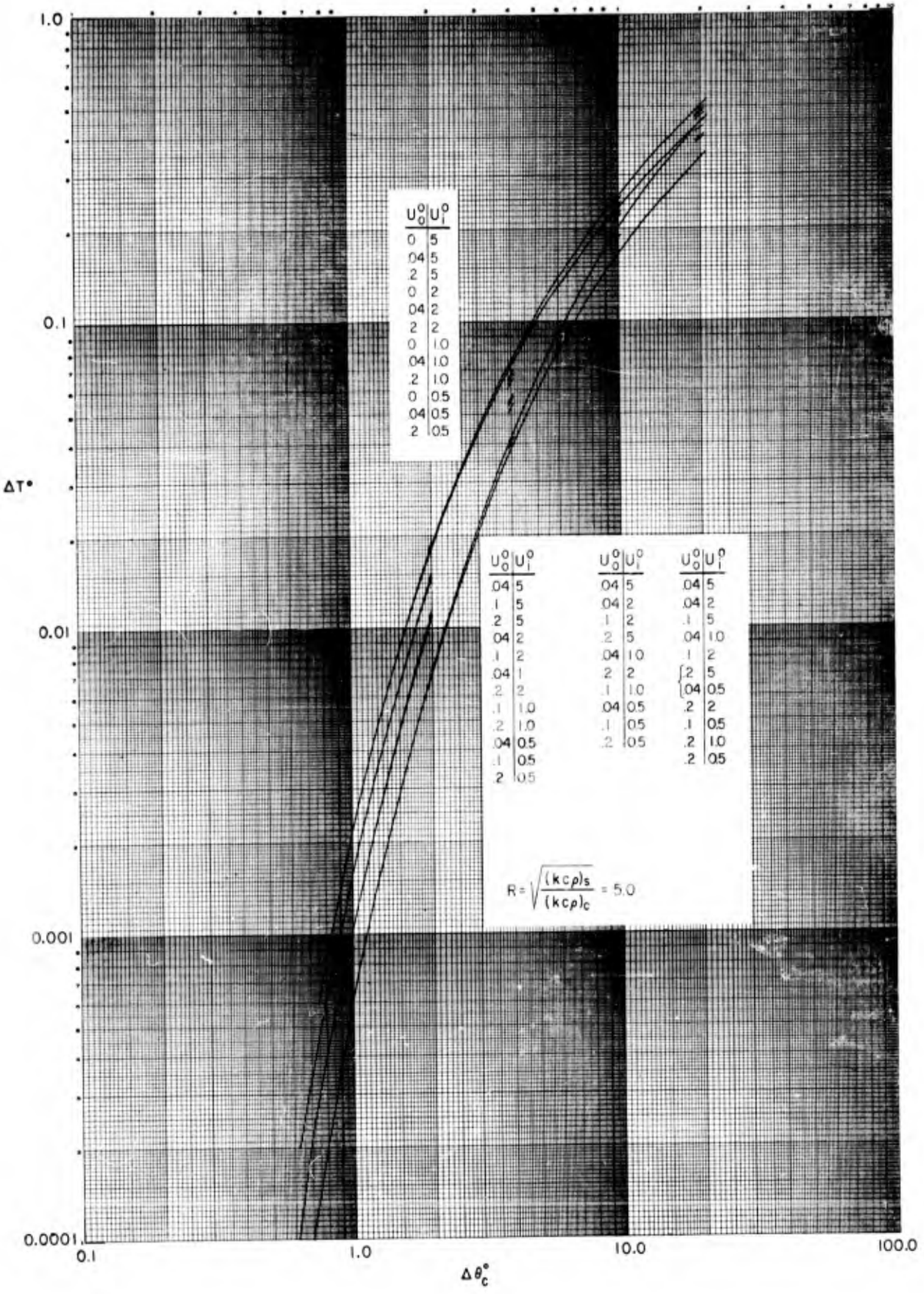

FIG.23 - TEMPERATURE HISTORY WITHIN AN OPAQUE SEMI-INFINITE SOLID (SKIN) FOLLOWING THERMAL IRRADIATION THROUGH AN OVERLYING CLOTH LAYER. $X^{o}_{s} = 0.55$
(Curve II - All radiation absorbed at $X^{o}_{c} = 0.75$)

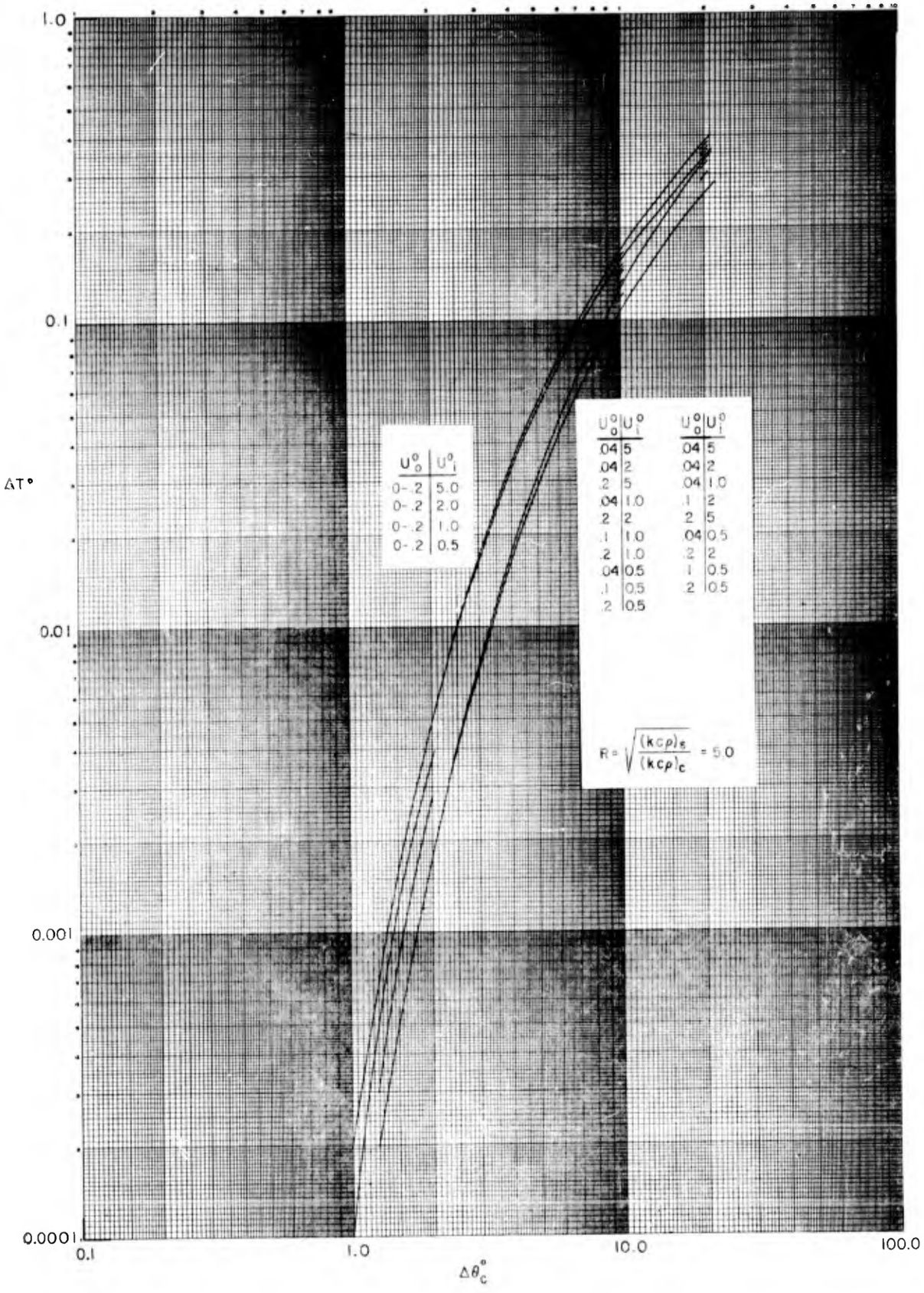

FIG.24 - TEMPERATURE HISTORY WITHIN AN OPAQUE SEMI-INFINITE SOLID (SKIN) FOLLOWING THERMAL IRRADIATION THROUGH AN OVERLYING CLOTH LAYER. $X_S^\circ = 0.75$
(Curve II - All radiation absorbed at $X_c^\circ = 0.75$)

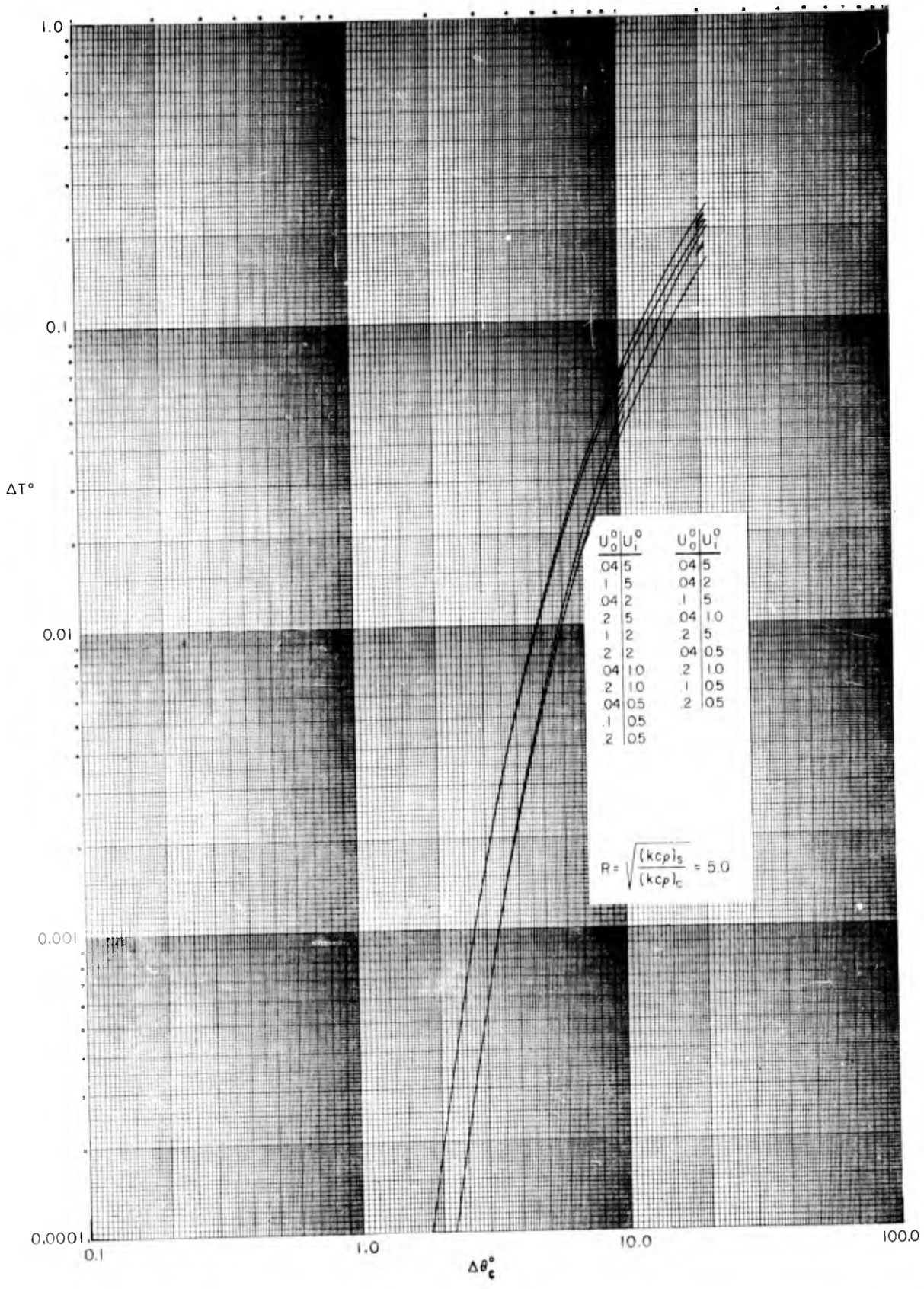

FIG. 25 - TEMPERATURE HISTORY WITHIN AN OPAQUE SEMI-INFINITE SOLID (SKIN) FOLLOWING THERMAL IRRADIATION THROUGH AN OVERLYING CLOTH LAYER. $X^{\circ}_{S} = 1.05$
(Curve II – All radiation absorbed at $X^{\circ}_{C} = 0.75$)

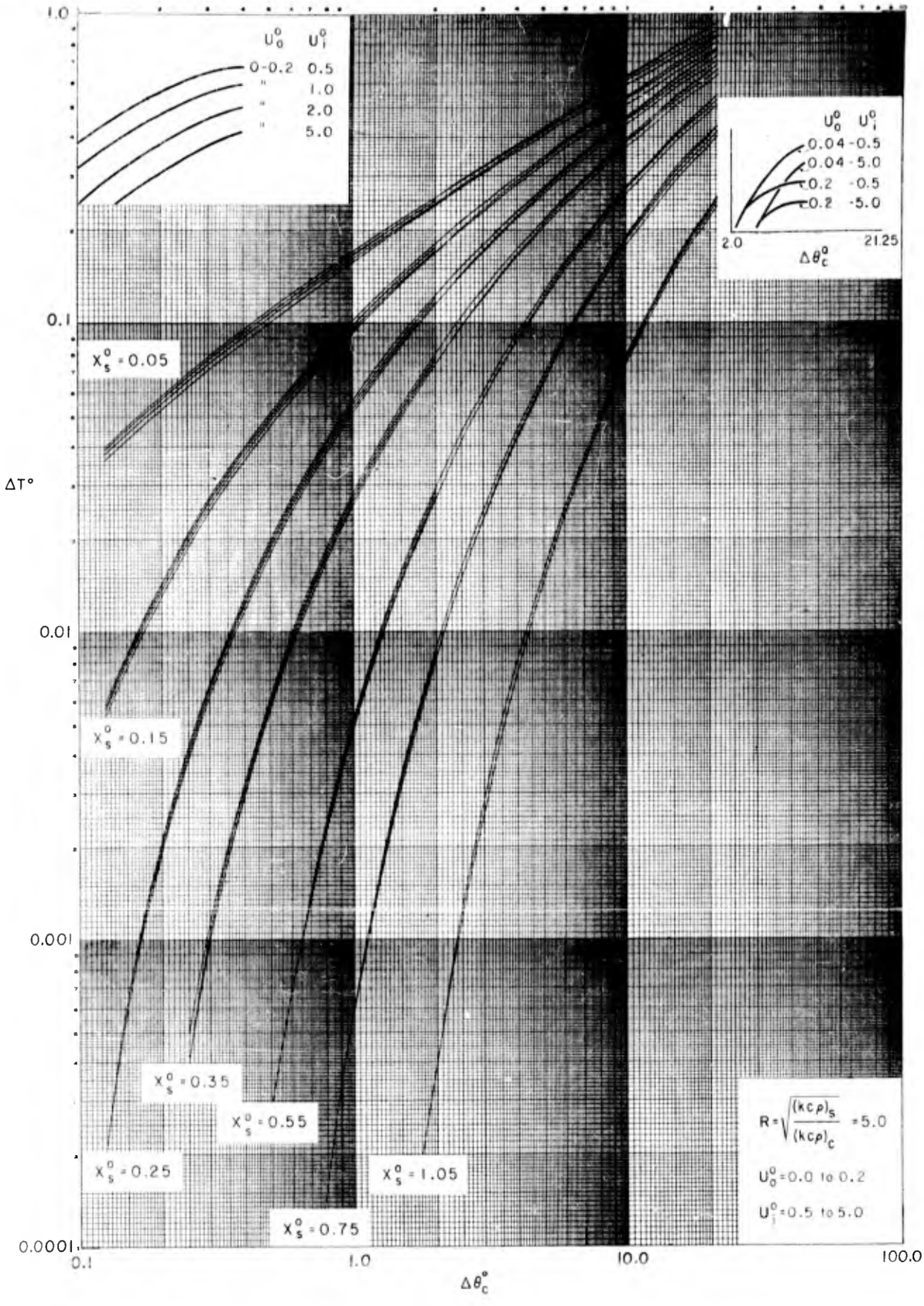

FIG. 26- TEMPERATURE HISTORY WITHIN AN OPAQUE SEMI-INFINITE SOLID (SKIN) FOLLOWING THERMAL IRRADIATION THROUGH AN OVERLYING CLOTH LAYER.
(Curve III- All radiation absorbed at skin surface)

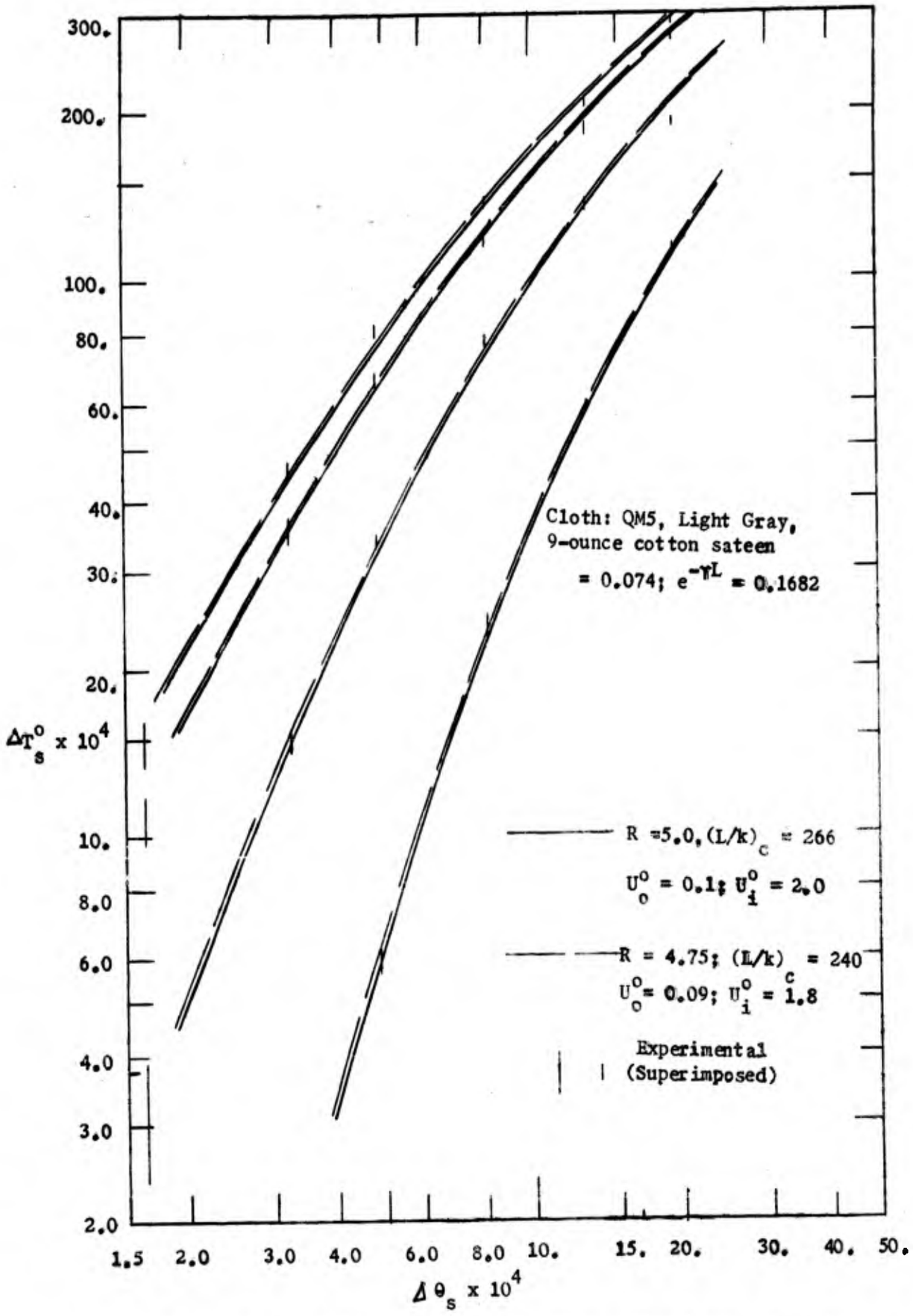

Fig. 27. Comparison of Theoretical and Experimental Temperature Histories Within a Skin Simulant Following Thermal Irradiation through Overlying Diathermanous Cloth.

DISTRIBUTION LIST FOR AFSWP TECHNICAL REPORTS

Massachusetts Institute of Technology

Technical Report No. 6

Heat Transfer to Skin through Thermally Irradiated Dry Cloth
Contract No. Nonr-1841(37) Project No. NRO51-237

No. of copies	Addressee
1	Asst. Chief of Staff, G-2 Department of the Army Washington 25, D.C.
1	Asst. Chief of Staff, G-3 Department of the Army Washington 25, D.C. Attn: Deputy Chief of Staff, G-3(RR&SW)
1	Asst. Chief of Staff, G-4 Department of the Army, W Washington 25, D.C.
1	Chief of Ordnance Department of the Army Washington 25, D.C. Attn: ORDTX-AR
3	Chief Signal Officer Department of the Army P & O Division Washington 25, D.C. Attn: SIGOP
1	The Surgeon General Department of the Army Washington 25, D.C. Attn: Chairman, Med R&D Board
2	Chief Chemical Officer Department of the Army Washington 25, D.C.
3	Asst. Chief of Engineers for Troop Operations OCE Department of the Army Washington, D.C.
2	The Quartermaster General, CBR, Liaison Office, R&D Div. Department of the Army Washington 25, D.C.

No. of Copies	Addressee
1	Chief of Transportation, Military Planning & Intelligence Department of the Army Washington 25, D.C.
4	Chief, Army Field Forces Fort Monroe, Virginia
1	President, Board #1, OCAFF Ft. Bragg, N.C.
1	President, Board #4, OCAFF Ft. Bliss, Texas
	Commanding General, First Army Governor's Island New York 4, New York
1	Attn: G-1
1	Attn: G-2
1	Attn: G-3
1	Attn: G-4
	Commanding General, Second Army Ft. George G. Meade, Md.
1	Attn: AIAME
1	Attn: AIACM
2	Commanding General, Third Army Ft. McPherson, Georgia Attn: AC ofS, G-3
1	Commanding General, Fourth Army Ft. Sam Houston, Texas Attn: G-3 Section
1	Commanding General, Fifth Army 1660 Hyde Park Blvd. Chicago 15, Illinois Attn: ALFEN
1	Commanding General, Sixth Army Presidio of San Francisco, California Attn: AMGCT-4
2	Commander-In-Chief, FECOM, APO 500 c/o PM San Francisco, California Attn: Ac of S. J-3
1	Commanding General, U.S. Army Alaska APO 942 c/o PM Seattle, Washington

No. of Copies	Addressee
3	Commanding General, US Army Forces Far East (Main) APO 343 c/o PM San Francisco, California Attn: AC of S, G-3
1	Commanding General, US Army Caribbean At. Amador, C.Z. Attn: Cml O
1	Commanding General, USARFATN & MDPR Ft. Prooke, Puerto Rico
2	Commanding General, US Army Pacific APO 958 c/o PM San Francisco, California Attn: Cml Off
1	Commandant, Command & General Staff College Ft. Leavenworth, Kansas Attn: ALLIS (AS)
1	Commandant, The Artillery School Ft. Sill, Oklahoma
2	Commandant, The Infantry School Ft. Benning, Georgia Attn: CDS
1	Commandant, The AA&GM Branch, The Artillery School Ft. Bliss, Texas
2	Commandant, The Armored School Ft. Know, Kentucky Attn: Class, Doc Sect, Eval & Res Div.
1	Commanding General, Medical Field Service School Brooke Army Medical Center Ft. Sam Houston, Texas
1	Director, Special Weapons Development Office, OCAFF Ft. Bliss, Texas
1	Commandant, Army Medical Service Graduate School Walter Reed Army Medical Center Washington 25, D.C. Attn: Dept. of Biophysics
1	The Superintendent, US Military Academy West Point, New York Attn: Professor of Ordnance

No. of Copies	Addressee
1	Commandant, Chemical Corps School Chemical Corps Training Command Ft. McClellan, Alabama
2	Commanding General, Research & Engineering Command Army Chemical Center, Maryland Attn: Special Projects Officer
2	RD Control Officer Aberdeen Proving Grounds, Maryland Attn: Dir. Ballistics Research Laboratory
3	Commanding General, The Engineer Center Ft. Belvoir, Virginia Attn: Asst. Cmdnt, Eng. School
1	Commanding Officer, Engineer Res. & Dev. Laboratory Ft. Belvoir, Virginia Attn: Chief, Tech Intelligence Branch
1	Commanding Officer, Picatinny Arsenal Dover, New Jersey Attn: ORDBB-TK
1	Commanding Officer, Frankford Arsenal, Ph Philadelphia 37, Pa. Attn: RD Control Officer
1	Commanding Officer, Army Medical Research Laboratory Ft. Knox, Kentucky
2	Commanding Officer, Chemical Corps Chemical and Radiological Laboratory Army Chemical Center, Maryland Attn: Tech. Library
1	Commanding Officer, Transportation R&D Station Ft. Eustis, Virginia
1	Chief, QM R&D Lab., Philadelphia QM Depot 2800 S. 20th St. Philadelphia 45, Pa. Attn: Mr. John Davies, Tech. Library
1	Director, Technical Documents Center Evans Signal Laboratory Belmar, New Jersey
1	Director, Waterways Experiment Station P.O. Box 631 Vicksburg, Miss. Attn: Library

No. of Copies	Addressee
1	Director, Operations Research Office John Hlpkins University 6410 Connecticut Avenue Chevy Chase, Maryland Attn: Library
2	Chief of Naval Operations Department of the Navy Washington 25, D.C. Attn: OP-36
1	Chief of Nval Operations Department of the Navy Washington 25, D.C. Attn: OP-374 (OBG)
2	Chief, Bureau of Medicine and Surgery Department of the Navy Washington 25, D.C. Attn: Special Weapons Defense Division
1	Chief, Bureau of Ordnance Department of the Navy Washington 25, D.C.
1	Chief of Naval Personnel Department of the Navy Washington 25, D.C. Attn: Pers C
2	Chief, Bureau of Ships Department of the Navy Washington 25, D.C. Attn: Code 348
1	Chief, Bureau of Supplies & Accounts Department of the Navy Washington 25, D.C.
1	Chief, Bureau of Yards & Docks Department of the Navy Washington 25, D.C.
2	Chief of Naval Research, Code 425 Rm 2501, Bldg T-3 Washington 25, D.C. Attn: Chemistry Branch
2	Office of Naval Research Branch Office Navy Bldg., 495 Summer St. Boston, Mass.

No. of Copies	Addressee
2	Commander-in-Chief, U.S. Atlantic Fleet U.S. Naval Base, Norfolk 11, Virginia
2	Commander-in-Chief, U.S. Pacific Fleet Fleet Post Office, San Francisco, California
4	Commandant, U.S. Marine Corps Washington 25, D.C. Attn: Code AO3H
1	President, U.S. Naval War College Newport, Rhode Island
1	Superintendent, U.S. Naval Postgraduate School Monterey, California
2	Commanding Officer, U.S. Naval Schools Command U.S. Naval Station Treasure Island San Francisco, California
	Director, USMC Development Center, USMD Schools Quantico, Virginia
1	Attn: Tactics Board
1	Attn: Equipment Board
2	Commanding Officer, U.S. Fleet Training Center Naval Base, Norfolk 11, Virginia Attn: Special Weapons School
2	Commanding Officer, U.S. Fleet Training Center Naval Station, San Diego 36, California Attn: (SPWP School)
1	Commanding Officer, Air Development Squadron 5, VX-5 U.S. Naval Air Station, Moffett Field, California
1	Commanding Officer, U.S. Naval Damage Control Training Center, Naval Base, Philadelphia 12, Pa. Attn: ABC Defense Course
1	Commanding Officer, U.S. Naval Unit, Chemical Corps School, Army Chemical Training Center Ft. McClellan, Alabama
	Commander, U.S. Naval Ordnance Laboratory White Oak, Maryland Silver Spring 19, Maryland
1	Attn: EE
2	Attn: R
1	Commander U.S. Naval Ordnance Test Station Inyokern, China Lake, California

No. of Copies	Addressee
2	Officer-in-Charge, U.S. Naval Civil Engineering Research & Evaluation Lab, U.S. Naval Construction Bn Center, Port Hueneme, California Attn: Code 753
1	Commanding Officer, U.S. Naval Medical Research Institute, National Naval Medical Center Bethesda 14, Maryland
1	Director, U.S. Naval Research Laboratory Washington 25, D.C.
1	Director, The Material Laboratory New York Naval Shipyard Brooklyn, New York
1	Commanding Officer & Director, U.S.N. Electronics Lab. San Diego, California Attn: Code 210
3	Commanding Officer, U.S.N. Radiological Defense Lab. San Francisco 24, California Attn: Tech. Info. Div.
1	Commanding Officer & Director David Taylor Model Basin Washington 7, D.C. Attn: Library
1	Commander, U.S.N. Air Development Center Johnsville, Pa.
2	Director, Office of Naval Research Branch Office 1000 Geary Street San Francisco, California
1	Officer-in-Charge, U.S.N. Clothing Factory U.S.N. Supply Activities New York 3rd Avenue & 29th Street Brooklyn 32, New York Attn: R&D Div.
1	Commanding Officer, Naval Medical Field Research Lab. Camp Lejeune, N.C.
1	Asst. for Atomic Energy, Hqs, USAF Washington 25, D.C. Attn: DCS/O
1	Asst. For Development Planning, Hqs, USAF Washington 25, D.C.

No. of Copies	Addressee
1	Director of Operations, Hqs, USAF Washington 25, D.C.
1	Director of Operations, Hqs, USAF Washington 25, D.C. Attn: Operations Analysis
1	Director of Plans, Hqs, USAF Washington 25, D.C. Attn: War Plans
1	Directorate of Requirements, Hqs, USAF Washington 25, D.C. Attn: AFDRQ-SA/M
1	Directorate of Research & Development Armament Division, DCS/D, Hqs, USAF Washington 25, D.C.
2	Directorate of Intelligence, Hqs, USAF Washington 25, D.C. Attn: AFOIN-1B2
1	The Surgeon General, Hqs, USAF Washington 25, D.C. Attn: Bio. Def. Br.
1	Commander, Far East Air Forces APO 925, c/o PM San Francisco
2	Alaskan Air Command APO 942, c/o PM Seattle, Wash. Attn: AAOTT
1	Commander, Northeast Air Command APO 862, c/o PM New York, N.Y.
1	Commander, Strategic Air Command Offutt AFB, Omaha, Nebraska Attn: Chief Operations Analysis
1	Commander, Tactical Air Command Langley AFB Virginia Attn: Doc Sec Br.
1	Commander, Air Defense Command Ent AFB, Colorado
	Commander, Air Materiel Command Wright-Patterson AFB Dayton, Ohio
2	Attn: MCAIDS
1	Attn: MCSW

No. of copies	Addressee
1	Commander, Air Training Command Scott AFB Belleville, Illinois Attn: DCS/O GTP
3	Commander, Air Research & Development Command P.O. Box 1395 Baltimore, Md. Attn: RDDN
1	Commander, Air Proving Ground Command Eglin AFB, Florida Attn: AG/TRB
2	Commander, Air University Maxwell AFB, Alabama
2	Commander, Air Command & Staff School Maxwell AFB, Alabama
2	Commander, Flying Training Air Force Waco, Texas Attn: Dir. of Observer Training
1	Commander, Crew Training Air Force Randolph AFB Randolph Field, Texas Attn: DCS/O, 2GTS
1	Commander, Headquarters Technical Training Air Force Gulfport, Miss. Attn: TA & D
2	Commander, Air Force School of Aviation Medicine Randolph AFB, Texas
1	Commander, Wright Air Development Center Wright-Patterson AFB Dayton, Ohio Attn: WC OESP
1	Commander, AF Cambridge Research Center 230 Albany Street Cambridge 39, Mass. Attn: Atomic Warfare Directorate
1	Attn: CRTSL-2
3	Commander, AF Special Weapons Center Kirtland AFB New Mexico Attn: Tech. Library

No. of copies	Addressee
1	Commander, USAF Institute of Technology Wright-Patterson AFB Dayton, Ohio Attn: Resident College
2	Commander, Lowry AFB Denver, Colo. Attn: Dept. of Armament Tng.
3	Commander, 1009th Special Weapons Squadron Hqs, USAF, Washington 25, D.C.
2	The RAND Corporation 1700 Main Street Santa Monica, California Attn: Nuclear Energy Division
1	Executive Secretary, Joint Chiefs of Staff Washington 25, D.C.
1	Director, Weapons Systems Evaluation Group, OSD Rm 2E1006, Pentagon Washington 25, D.C.
1	Asst. for Civil Defense, OSD Washington 25, D.C.
1	Chairman, Armed Services Explosives Safety Board DOD, Room 2403, Barton Hall Washington 25, D.C.
1	Executive Secretary, Military Liaison Committee P.O. Box 1814 Washington 25, D.C.
1	U.S. National Military Representative Headquarters SHAPE APO 55, c/o PM New York, N.Y. Attn: Col. J.P. Healy
1	Asst. Secretary of Defense for Research & Development DOD Washington 25, D.C. Attn: Tech. Library
1	Commandant, Armed Forces Staff College Norfolk 11, Va. Attn: Secy.

No. of copies	Addressee
6	Commanding General, Field Command AFSWP P.O. Box 5100 Albuquerque, New Mexico
5	ASTIA Document Service Center Arlington Hall Station Arlington 12, Virginia
1	Dr. H. C. Hottel Massachusetts Institute of Technology Cambridge 39, Mass.
1	Dr. E. O. Hulbert Naval Research Laboratory Washington 25, D.C.
1	Dr. H. E. Pearse Strong Memorial Hospital 260 Crittenden Blvd. University of Rochester Rochester 7, New York
1	Dr. J. D. Hardy Department of Physiology Cornell University Medical College 1300 York Avenue New York 21, N.Y.
1	Dr. R. P. Peterson Applied Physics Division Sandia Corporation Albuquerque, New Mexico
1	Dr. Alvin C. Graves Los Alamos Scientific Laboratory Box 1663, Los Alamos, New Mexico
1	Dr. Alan R. Moritz or D. A. Axelrod Institute of Pathology 2085 Adelbert Road Cleveland 6, Ohio
1	University of California, Engineering Research P.O. Box 4063, Westwood Village Station Los Angeles 24, California
50	Headquarters, Quartermaster R and D Command Research and Development Center Pioneering Research Division Natick, Massachusetts Attn: Mr. John M. Davies, Special Projects Branch

No. of copies	
1	Commanding Officer Diamond Ordnance Fuze Laboratories Wash. 25, D.C. Attn: Technical Reference Section (ORDTL 06.33)
1	U.S. Army Chemical Warfare Laboratories Technical Library Army Chemical Center, Maryland
3	Chief, AFSWP Attn: Document Library Branch Washington 25, D.C.